Peer-reviewed version available at Appl. Sci. 2019, 9, 527; doi:10.3390/app9030527

Article

Analytical Solutions for the Propagation of UltraShort and UltraSharp Pulses in Dispersive Media

Er'el Granot[1,*]

[1] Department of Electrical and Electronic Engineering, Ariel University, Ariel, Israel; erel@ariel.ac.il
* Correspondence: erelgranot@gmail.com

Abstract: Ultrashort pulses are severely distorted even by low dispersive media. While the mathematical analysis of dispersion is well known, the technical literature focuses on pulses, which keep their shape: Gaussian and Airy pulses. However, the cases where the shape of the pulse is unaffected by dispersion is the exception rather than the norm. It is the object of this chapter to present a variety of pulses profiles, which have analytical expressions but can simulate real-physical pulses with greater accuracy. In particular, the dynamics of smooth rectangular pulses, physical Nyquist-Sinc pulses, and slowly rising but sharply decaying ones (and vice-versa) are presented. Besides the usage of this chapter as a handbook of analytical expressions for pulses' propagations in a dispersive medium, there are several new findings. The main ones are: Analytical expressions for the propagation of chirped rectangular pulses, which converge to extremely short pulses; analytical approximation for the propagation of Super-Gaussian pulses; the propagation of Nyquist Sinc Pulse with smooth spectral boundaries and an analytical expression for a physical realization of an attenuation compensating Airy pulse.

Keywords: Ultrashort pulses, Dispersion, Pulse distortion, optical communications

1. Introduction

Ultrashort pulses are ubiquitous in numerous applications: In bio- and medical-imaging (see, for example, [1-3]), optical communications (see, for example, [4,5]), microscopy (see, for example, [6,7)], etc.

One of the clear shortcomings of short pulses is the consequences of their wide spectrum. When the spectrum is spectrally wide, the absorption variations within the spectrum increases. However, even if the absorption is approximately homogenous within the pulse spectral range, the refraction index is wavelength dependent and therefore the pulse experiences dispersion effects.

Dispersion occurs whenever each one of the pulse's spectral components propagates with a different velocity. Consequently, the pulse experiences shape distortions. The temporally shorter the pulse, the larger are the distortions. Moreover, while the dispersion effects are proportional to the medium's length, it is inversely proportional to the square of the pulse's temporal width; therefore, ultra-short pulses are prone to be affected by dispersion even in relatively short media[8-10].

Clearly, most of the dispersion mitigation techniques were implemented in the optical communication arena, where dispersion can have a destructive effect on the transmitting signals. It has been shown that via ordinary smf28 fiber (the most ubiquitous fiber type) it is impossible to decode data, which is transmitted at a 10Gb/s rate, beyond a distance of 160km (see Ref.[11] and in the quantum analogy see Ref.[12]). Clearly, in the presence of noise, this distance shrinks substantially. If the data is carried by picosecond pulses (which is only 1% of the temporal width of the 10Gb/s signal's individual pulses) this maximum distance is reduced to merely 16m, and the distortion effects will be felt within less than a meter. In the femtosecond domain, the dispersion effects are, using the terminology and example of Ref.[13], more dramatic: a 10fs laser pulse in the 800nm spectral regime, which propagate through a 4mm of BK7 glass will be temporally broadened to 50fs!

It is well known that dispersion is governed by the dispersion equation, which can easily be solved numerically. However, to evaluate the effects of dispersion and to predict them, some intuition is required. In most textbooks, Gaussian pulses are used as a litmus tool to predict the dispersion effect[8,13,14]. Gaussian pulses are very useful since, on the one hand, they are localized pulses with a well-defined width and energy, and on the other hand, the shape of their spectrum is mathematically similar to the dispersion effect. Therefore, the propagation of Gaussian pulses in dispersion medium has a relatively simple analytical solution. This simple pulse model can be used to evaluate *qualitatively* some fundamental limitations. However, it fails in quantifying their values (see Ref.[11] and references therein). In fact, the Gaussian model predicts that the pulse keeps its Gaussian shape, and its width is proportional to the square root of the elapsed period. This conduct resembles the spatial spreading of a Gaussian distribution of particles in a diffusion process[15]. Since the "particle" realization of the dispersion process is common in the popular description of chromatic dispersion, the similarity to diffusion may be misleading, since, in fact, this similarity appears only in the Gaussian scenario. Whenever the initial pulse profile deviates from the Gaussian's one, the differences between diffusion and dispersion are clearly shown. In general, the two processes tend to smooth out the signal. However, the processes are fundamentally different, and the main differences appear after short distances. This discrepancy clearly appears in most optical communication protocols, where the pulses never have Gaussian profiles. Consequently, the signal distortion is completely different from the Gaussian analysis predictions. To overcome this problem, super Gaussian pulses are commonly used to model real communications scenarios [16-18]. Despite the fact that super Gaussian are much better approximation to real pulses, they have two weaknesses: they cannot be implemented in Non-Return-to-Zero (NRZ) protocols and they do not have a close-form analytical solution.

It is the object of this chapter to assemble important pulses profile, whose propagation in dispersive medium can be expressed in analytical terms. It is shown that there are profiles, which are much better candidates to simulate real pulses, but their dynamics can be formulated in a closed-form analytical expressions.

Moreover, it is shown that the dynamics of almost any practical pulse profile in dispersive media can be simulated and approximated by analytical expressions.

In the 1st part of the chapter, after the introduction of the general theory (sec.2) and the presentation of fundamental theorems (sec.3), the propagation of a Gaussian pulse is presented (sec. 4). In the 2nd part, it is shown that it is possible to present analytically the propagation of singular pulses (sec. 5), which can be written initially with exponentials and step functions (like rectangular pulses and exponential-step pulses). In the 3rd part it is shown that every step function can be replaced with a smooth step function, and therefore, any singular

pulse, which is presented in the previous part, can be replaced with its counterpart smooth version (sec. 6). In particular, smooth rectangular pulses can replace super Gaussian ones. The 4th part is dedicated to the important pulse, which is singular in the spectral domain, i.e., the Nyquist-Sinc pulse (sec. 7). First the analytical expression for its propagation in dispersive medium is presented, and then the analytical expression of the propagation of its spectrally-smooth, i.e., physical, counterpart is presented as well. In the last part of the chapter, accelerated-airy pulses and attenuation compensating pulses are presented, as well as their physical counterparts (sec 8).

2. Generic Dispersion Analysis

Let $A(t,z)$ represents the envelope of an electromagnetic (EM) pulse, which propagates in the z-direction in a dispersive medium with the dispersion coefficient β_2, then $A(t,z)$ obeys the following equation [14]

$$i\frac{\partial A(t,z)}{\partial z}=\frac{\beta_2}{2}\frac{\partial^2 A(t,z)}{\partial t^2} \tag{1}$$

where $t=t'-z/v$ is the time in a frame of reference that travels at the velocity of light in the medium ($v=c/n$, where c is the vacuum light's velocity and n is the mean refractive index), i.e., t' is the real time. This equation is valid provided all spectral components of the pulse are governed by the following dispersion relation

$$\frac{n}{c}\omega+\frac{\beta_2}{2}\omega^2=k \tag{2}$$

If $A(t,0)$ is the initial pulse profile, then the pulse profile at the end of the medium $A(t,z)$ can be evaluated by the following convolution

$$A(t,z)=\int_{-\infty}^{\infty}K(t-t',z)A(t',0)dt' \tag{3}$$

where the dispersion Kernel (see Appendix A) is

$$K(t-t',z)=(-2\pi i\beta_2 z)^{-1/2}\exp\left(-i\frac{(t-t')^2}{2\beta_2 z}\right) \tag{4}$$

3. Fundamental Dispersion Theorems

To analyze the dispersion dynamics of the different pulses, we need some analytical tools, which will be formulated as the following theorems.

3.1. Pulse Boosting and Decaying

Let $A(t,0)$ be an initial pulse whose dispersive dynamics is known, i.e., at the end of the dispersive medium its profile is also given $A(t,z)$. Then, if the initial pulse is boosted by shifting the pulse's spectrum, i.e., by multiplying the profile by an harmonic function

$$A'(t,z=0)=\exp(i\omega_0 t)A(t,0) \tag{5}$$

then the pulse's profile at the end of the medium (after a distance z) is (see Appendix B)

Preprints (www.preprints.org) | NOT PEER-REVIEWED | Posted: 20 January 2019 doi:10.20944/preprints201901.0191.v1

Peer-reviewed version available at Appl. Sci. 2019, 9, 527; doi:10.3390/app9030527

$$A'(t,z>0)=\exp\left(i\frac{\beta_2}{2}\omega_0^2 z+i\omega_0 t\right)A(t+\beta_2\omega_0 z,z). \quad (6)$$

Clearly, this theorem can be generalized to the case where the initial pulse is multiplied by an exponent

$$A'(t,z=0)=\exp(at)A(t,0) \quad (7)$$

where a can be any real, imaginary or complex number. In which case, if the initial function does no diverge, the solution at the end of the medium is

$$A'(t,z>0)=\exp\left(-i\frac{\beta_2}{2}a^2 z+at\right)A(t-i\beta_2 az,z) \quad (8)$$

3.2 Pulse Chirping

Let $A(t,0)$ be an initial pulse whose dispersive dynamics is known, i.e., at the end of the dispersive medium its profile is $A(t,z)$, then, if the initial pulse is chirped, i.e.,

$$A'(t,0)=\exp(-iqt^2)A(t,0) \quad (9)$$

for any real q, the pulse's profile at the end of the medium (after a distance z) is (see Appendix C)

$$A'(t,z)=(1+2\beta_2 zq)^{-1/2}\exp\left(-i\frac{t^2}{2\beta_2 z+1/q}\right)A\left(\frac{t}{1+2\beta_2 zq},\frac{z}{1+2\beta_2 zq}\right). \quad (10)$$

Again, this theorem can be generalized to the case where the initial profile is multiplied by a generic Gaussian. That is, if the initial pulse is

$$A'(t,0)=\exp(-qt^2)A(t,0), \quad (11)$$

where q can be any complex number, then as long as $\Re q>0$, the solution at the end of the medium is

$$A'(t,z)=(1-i2\beta_2 zq)^{-1/2}\exp\left(-i\frac{t^2}{2\beta_2 z+i/q}\right)A\left(\frac{t}{1-i2\beta_2 zq},\frac{z}{1-i2\beta_2 zq}\right) \quad (12)$$

4. Gaussian Pulse

The simplest pulse, which is ubiquitous in the literature, is the Gaussian one. This is one of the few cases where the pulse has the same shape as its Fourier Transform. Therefore, since the dispersion dynamics can be formulated as a convolution with a complex Gaussian (4), then in general the pulse profile remains a complex Gaussian. In this case, the initial pulse profile is

$$A(t,0)=A_0\exp\left(-(t/\theta)^2\right) \quad (13)$$

and thus the pulse's profile at the end of the dispersive medium is (following Eq.(12))

$$A(t,z)=\frac{A_0\theta}{\sqrt{\theta^2-2i\beta_2 z}}\exp\left(-\frac{1}{\theta^2-2i\beta_2 z}t^2\right). \quad (14)$$

The profile of Eq.(14) is plotted in Fig.1 and a spatiotemporal presentation of its intensity $|A(t,z)|^2$ is presented in Fig.2. Hereinafter we adopt the following dimensionless parameters:

Preprints (www.preprints.org) | NOT PEER-REVIEWED | Posted: 20 January 2019 doi:10.20944/preprints201901.0191.v1

Peer-reviewed version available at Appl. Sci. 2019, 9, 527; doi:10.3390/app9030527

141 $\tau \equiv t/\theta$ and $\zeta \equiv \beta_2 z/\theta^2$.

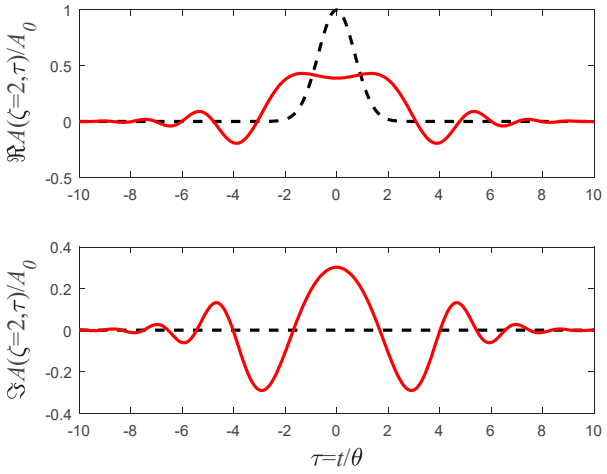

142

143 Fig.1: The real (upper panel) and imaginary (lower panel) components of the pulse (14). The dashed curve

144 represents the initial profile (for $\zeta = \beta_2 z/\theta^2 = 0$), while the solid curve represents the signal after a distance,

145 which corresponds to $\zeta = \beta_2 z/\theta^2 = 2$. Time is measured in units of θ, which corresponds to the pulse's

146 temporal width.

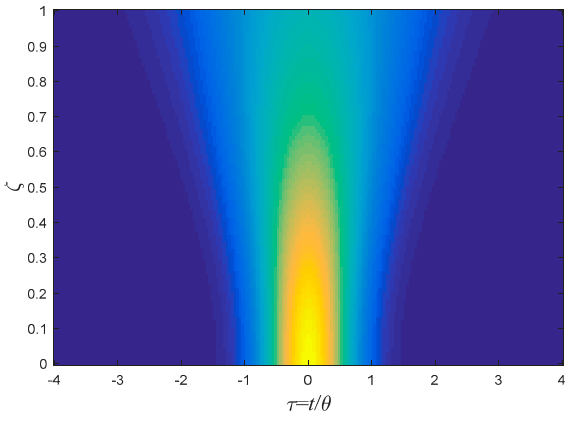

147

148 Fig.2: A false-color presentation of the pulse's intensity $|A(t,z)|^2$ (Eq.(14)) as a function of the normalized time

149 $\tau \equiv t/\theta$ and the normalized distance $\zeta \equiv \beta_2 z/\theta^2$.

150

151 Sample Application: The pulses that many mode locked lasers emit can be simulated by Gaussian pulses (see

152 [14]). When such a pulse with a FWHM of 1ps (which corresponds to $\theta = FWHM/\sqrt{\ln 4} \cong 0.85ps$) and a

Preprints (www.preprints.org) | NOT PEER-REVIEWED | Posted: 20 January 2019 doi:10.20944/preprints201901.0191.v1

Peer-reviewed version available at Appl. Sci. 2019, 9, 527; doi:10.3390/app9030527

carrier wavelength of $\lambda = 1.06\mu m$ enters a BK7 glass, then $|\beta_2| \cong 24 ps^2/Km$, and $\zeta = 1$ in Fig. 2 corresponds to $z = \zeta\theta^2/\beta_2 \cong 30m$.

4.2 Boosted Gaussian

When the initial pulse is a boosted Gaussian

$$A(t, z=0) = A_0 \exp\left(-t^2/\theta^2 + i\omega_0 t\right) \tag{15}$$

then using relation (6), the final profile is

$$A(t,z) = \frac{A_0\theta}{\sqrt{\theta^2 - 2i\beta_2 z}} \exp\left(i\frac{\beta_2}{2}\omega_0^2 z + i\omega_0 t\right) \exp\left(-\frac{(t+\beta_2\omega_0 z)^2}{\theta^2 - 2i\beta_2 z}\right) \tag{16}$$

which means that beside the pulse spreading, the pulse's peak propagates with reciprocal "velocity" $\beta_2\omega_0$. The larger the spectral shift ω_0 the larger is the temporal shift of the pulse. The pulse's profile and its intensity's dynamics are presented in Figs.3 and 4 respectively.

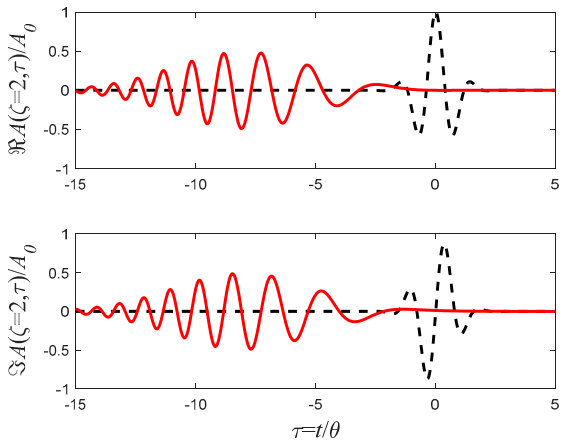

Fig.3: The real (upper panel) and imaginary (lower panel) components of the Gaussian pulse (16). The dashed curve represents the initial profile (for $\zeta = \beta_2 z/\theta^2 = 0$), while the solid curve represents its final shape (for $\zeta = \beta_2 z/\theta^2 = 2$),. In this example, the carrier frequency is $\omega_0 = -4/\theta$.

Preprints (www.preprints.org) | NOT PEER-REVIEWED | Posted: 20 January 2019 doi:10.20944/preprints201901.0191.v1

Peer-reviewed version available at Appl. Sci. 2019, 9, 527; doi:10.3390/app9030527

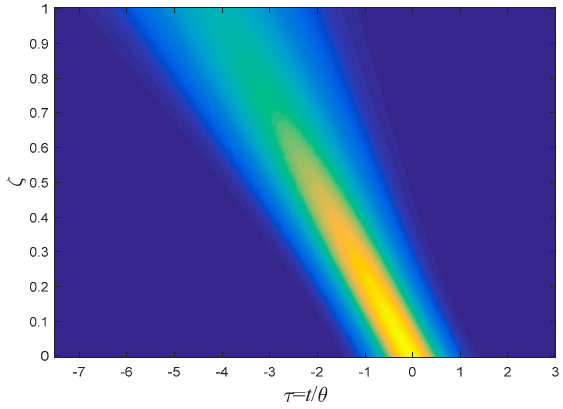

Fig.4: Same as Fig.2 but for the intensity ($|A(t,z)|^2$) of the pulse presented by Eq.(16) (in this example $\omega_0 = -4/\theta$).

4.3 Chirped Gaussian

When the initial pulse is chirped, i.e., the pulse's phase has an additional quadratic dependence on time, i.e.,

$$A(t,0) = A_0 \exp\left(-\frac{t^2}{\theta^2} - iqt^2\right) \tag{17}$$

then, using Eq.(10) the final pulse is

$$A(t,z) = \frac{A_0}{\sqrt{1+2\beta_2 z(q-i/\theta^2)}} \exp\left(-\frac{t^2}{\theta^2}\left[\frac{iq\theta^2+1}{1+2\beta_2 z(q-i\theta^{-2})}\right]\right) \tag{18}$$

In Fig. 18 the temporal dynamics of the pulse (18) is presented for the same parameters as Fig.2 but with additional $q = -2/\theta^2$. The shrinkage of the pulse's width is clearly shown, which is a consequence of the fact that the chirping has widened the spectral width of the initial pulse.

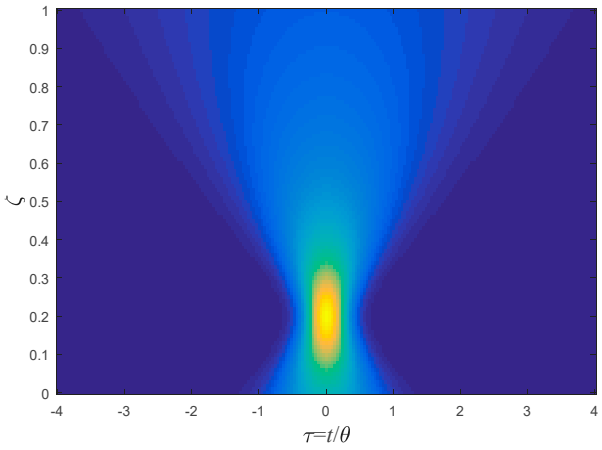

Fig.5 Same as Fig.2 but for the intensity ($|A(t,z)|^2$) of the pulse presented by Eq.(18) (in this example $q = -2/\theta^2$).

5. Singular Pulses

Before going into the propagation of profiles, which can simulate *real* pulses, it is instructive to investigate a family of pulses with singularity points. The singularity points are points, in which either the pulse's amplitude or its derivatives are discontinuous. Despite their singularities, these pulses can simulate pulses, which have sharp boundaries. Moreover, it will be shown that these generalized, i.e., singular, pulses can be modified very simply into smooth ones, and therefore can be implemented in real, physical scenarios.

5.1 The Step Function

The step function response of a dispersive medium is related to the complex error function.

Let the initial pulse's profile be a step function, i.e.,

$$A(z=0,t)=A_0u(-t) \tag{19}$$

where $u(t)=\begin{cases}1 & t>0\\ 0 & t\le 0\end{cases}$ is the Heaviside step-function, then, the pulse at the end of the medium is

$$A(t,z)=A_0\int_{-\infty}^{0}(-2\pi i\beta_2 z)^{-1/2}\exp\left(-i\frac{(t-t')^2}{2\beta_2 z}\right)dt'=\frac{1}{2}A_0 erfc\left(\frac{t}{\sqrt{-2i\beta_2 z}}\right). \tag{20}$$

Clearly, if initially

$$A(z=0,t)=A_0u(-t+T) \tag{21}$$

then

$$A(t,z)=\frac{1}{2}A_0 erfc\left(\frac{t-T}{\sqrt{-2i\beta_2 z}}\right). \tag{22}$$

Similarly, using (6) the initial boosted step function pulse

$$A(t,z=0)=A_0\exp(i\omega_0 t)u(-t+T) \tag{23}$$

will propagates to read

$$A(t,z>0)=\frac{1}{2}A_0\exp\left(i\frac{\beta_2}{2}\omega_0^2 z+i\omega_0 t\right)erfc\left(\frac{t-T+\beta_2\omega_0 z}{\sqrt{-2i\beta_2 z}}\right). \tag{24}$$

This result is known in the literature as Moshinsky's function. In Quantum Mechanics, this function was used to simulate an electrons' beam, which was blocked by a beam shutter[19,20]. In the Quantum analogy, the wavefunction exhibits interference in time.

5.2 Rectangular Pulses

The fundamental generalized pulse is the rectangular one. Unlike the delta function, the rectangular pulse has a finite energy, and therefore can simulate in many scenarios, despite its singular edges, a real rectangular pulse, and therefore it is ubiquitous in the literature.

Preprints (www.preprints.org) | NOT PEER-REVIEWED | Posted: 20 January 2019 doi:10.20944/preprints201901.0191.v1

Peer-reviewed version available at Appl. Sci. 2019, 9, 527; doi:10.3390/app9030527

The rectangular pulse can be written with the aid of the step function or the rectangular function

$$A(z=0,t)=A_0 rect_1(t/\theta)=A_0\left[u(-t/\theta+0.5)-u(-t/\theta-0.5)\right] \tag{25}$$

where

$$\mathrm{rect}_L(\tau)\equiv\begin{cases}1 & |\tau|\le L/2\\ 0 & |\tau|>L/2\end{cases}. \tag{26}$$

Eq.(25) has two singular points ($t=\pm 0.5\theta$), in which the pulse's amplitude is discontinuous.

The dynamics of this rectangular pulse can be formulated analytically

$$A(t,z)=\frac{1}{2}A_0\left[erfc\left(\frac{t-\theta/2}{\sqrt{-2i\beta_2 z}}\right)-erfc\left(\frac{t+\theta/2}{\sqrt{-2i\beta_2 z}}\right)\right]. \tag{27}$$

In Fig.6 the real and imaginary components of (27) are plotted for two different medium's length. The ripples in the pulse's profile appear after a very short distance.

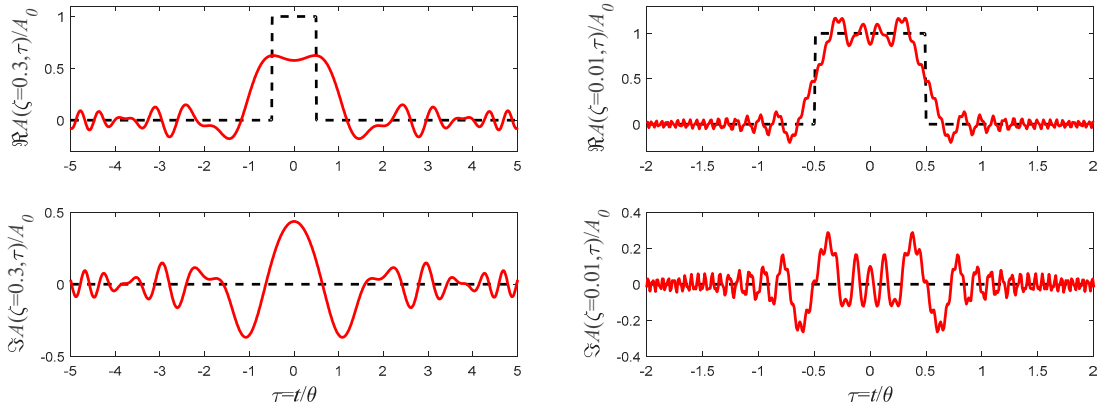

Fig.6: The real (upper panel) and imaginary (lower panel) components of the rectangular pulse (27). The dashed curve represents the initial profile (for $\zeta=\beta_2 z/\theta^2=0$), while the solid curve represents its final shape (for $\zeta=\beta_2 z/\theta^2=0.01$ on the right and $\zeta=\beta_2 z/\theta^2=0.3$ on the left).

In Fig.7 a spatiotemporal intensity plot (as a function of τ and ζ) is presented.

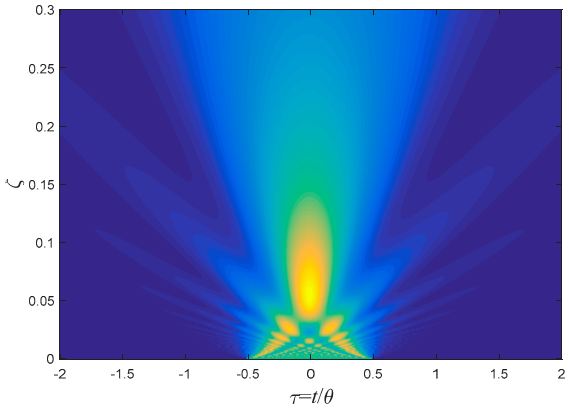

Fig.7: Same as Fig.2 but for the intensity ($|A(t,z)|^2$) of the pulse presented by Eq.(27)

The intricate structure of this function is most pronounced when the incident signal is a train of rectangular pulses

$$A(z=0,t)=A_0\sum_{n=-\infty}^{\infty} rect_1(t/\theta-2n). \qquad (28)$$

This case is equivalent to the well-known quantum problem of a particle in a 1D box, when initially the particle's probability density is uniform over the box [21].

In this case the problem's dynamics can be formulated [using (27)] by

$$A(t,z)=\frac{1}{2}A_0\sum_{n=-\infty}^{\infty}\left[erfc\left(\frac{t-2n-\theta/2}{\sqrt{-2i\beta_2 z}}\right)-erfc\left(\frac{t-2n+\theta/2}{\sqrt{-2i\beta_2 z}}\right)\right]. \qquad (29)$$

However, it should be emphasized, that in Ref.[21] a different numerical approach was taken, in which no error function analysis was used.

Sample Application: In 10Gb/s optical communications channel (over smf28 fiber) with a carrier wavelength of $\lambda=1.55\mu m$, the pulses can be simulated by rectangular ones with $\theta=100ps$ and $\beta_2\cong 20ps^2/Km$, in which case $\zeta=0.3$ in Fig.7 corresponds to $z=\zeta\theta^2/\beta_2\cong 150Km$. However, as Fig.6 illustrates, considerable distortions appear even for $\zeta=0.01$, which corresponds to a fiber length of $z\cong 5Km$.

5.3 Chirped Rectangular Pulses

One of the methods to combat dispersion in optical communication is to chirp the pulses, and since most pulses in optical communications are rectangular (in fact they are smooth rectangular, see below) it is instructive to investigate analytically the dynamics of a chirped rectangular pulse.

Preprints (www.preprints.org) | NOT PEER-REVIEWED | Posted: 20 January 2019 doi:10.20944/preprints201901.0191.v1

Peer-reviewed version available at Appl. Sci. 2019, 9, 527; doi:10.3390/app9030527

The initial chirped rectangular pulse has the following form

$$A(0,t)=A_0\exp\left(-iqt^2\right)rect_1(t/\theta)=A_0\exp\left(-iqt^2\right)\left[u(-t/\theta+0.5)-u(-t/\theta-0.5)\right]. \quad (30)$$

Therefore, using (10) and (24), the pulse profile after a distance z is

$$A(z>0,t)=\exp\left(\frac{-iqt^2}{2\beta_2 zq+1}\right)\frac{A_0}{2\sqrt{1+2\beta_2 zq}}\left[erfc\left(\frac{t-\theta(1+2\beta_2 zq)/2}{\sqrt{-2i\beta_2 z(1+2\beta_2 zq)}}\right)-erfc\left(\frac{t+\theta(1+2\beta_2 zq)/2}{\sqrt{-2i\beta_2 z(1+2\beta_2 zq)}}\right)\right] \quad (31)$$

Besides the widening of the pulse's boundaries, the boundaries also moves at a constant "velocity", i.e., the two boundaries obey the following relationship

$$t_B=\pm\frac{\theta}{2}(1+2\beta_2 qz) \quad (32)$$

Clearly, when q is positive, the two boundaries collide at a distance

$$z_f=-1/2\beta_2 q\,, \quad (33)$$

which is independent of the pulse's width θ. In Fig. 8 the propagation of this pulse for both positive and negative q is presented.

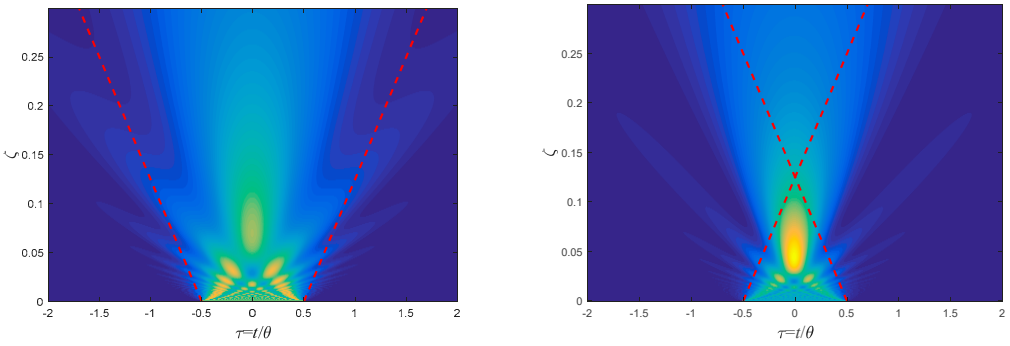

Fig.8: Same as Fig.2 but for the intensity ($|A(t,z)|^2$) of the pulse presented by Eq.(31). On the left $q=4/\theta^2$, and on the right $q=-4/\theta^2$. The dashed lines corresponds to the pulse's boundaries $t_B=\pm\theta(1+2\beta_2 qz)/2$.

While the pulse indeed shrinks for negative q, the pulse's minimum width is reached before the distance z_f, i.e. Eq.(33). However, if the two pulses are combined, i.e., if the initial pulse is

$$A(z=0,t)=A_0\cos\left(qt^2\right)rect_1(t/\theta)=A_0\cos\left(qt^2\right)\left[u(-t/\theta+0.5)-u(-t/\theta-0.5)\right] \quad (34)$$

then the minimum width occurs exactly at the distance z_f. In Fig. 9 the temporal dynamics of this pulse is presented, and the point z_f is clearly shown. Clearly, a smoother, i.e., more realistic, pulse will not converge to an infinitely temporally narrow pulse, but instead will converge to a finite temporal width.

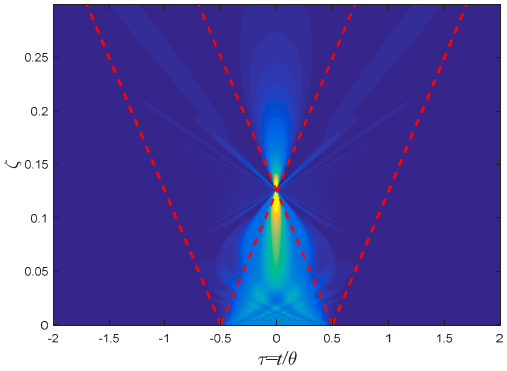

Fig.9: Same as Fig.8 but with the initial pulse Eq.(34) for the parameter $q = 4/\theta^2$.

5.4 Exponential Pulse

The product of the step function with the exponential function allows investigating the dynamics of the simplest exponential function. Utilizing (8), the initial exponential-step function

$$A(t, z=0) = A_0 \exp(at) A(t,0) \tag{35}$$

will propagate in dispersive medium according to

$$A(z>0,t) = \frac{A_0}{2} \exp\left(-i\frac{\beta_2}{2}a^2 z + at\right) erfc\left(\frac{t - i\beta_2 az}{\sqrt{-2i\beta_2 z}}\right). \tag{36}$$

In Fig.10 the dynamics of the exponential-step function pulse is plotted.

A spatiotemporal presentation of the pulse's intensity is presented in Fig.11. This pulse can simulate a pulse where its rise time is considerably shorter than its decay time. In both figures $a = 1/\theta$.

Preprints (www.preprints.org) | NOT PEER-REVIEWED | Posted: 20 January 2019 doi:10.20944/preprints201901.0191.v1

Peer-reviewed version available at Appl. Sci. 2019, 9, 527; doi:10.3390/app9030527

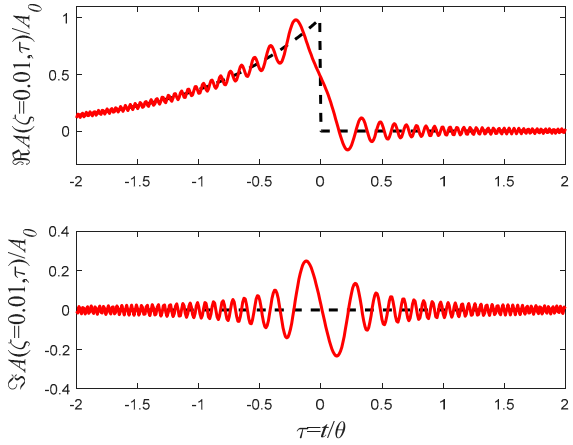

Fig.10: The real (upper panel) and imaginary (lower panel) components of the exponential-step function pulse (36). The dashed curve represents the initial profile (for $\zeta=\beta_2 z/\theta^2=0$), while the solid curve represents its final shape (for $\zeta=\beta_2 z/\theta^2=0.01$).

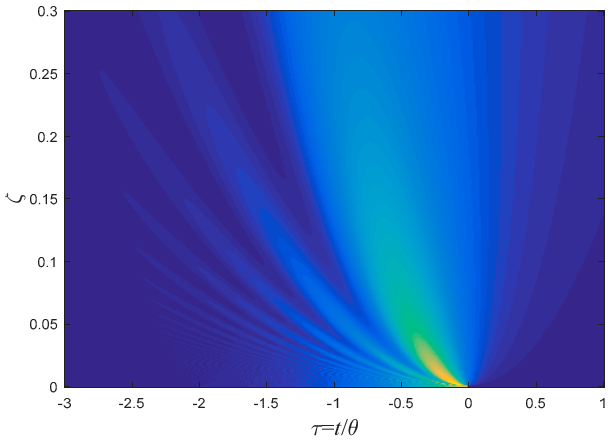

Fig.11: Same as Fig.2 but for the intensity ($|A(t,z)|^2$) of the pulse presented by Eq.(36).

5.5 Cosine Pulse

A bounded cosine pulse is an example of a continuous pulse (unlike the rectangular one), where the discontinuity at the edges of the pulse occurs on the amplitude's derivative level.

It should be stressed that in terms of the pulse's *intensity*, the derivative is continuous as well. Therefore, this is an important pulse, because for many practical purposes, it mimics a continuous pulse, but at the same time, it is (initially) temporally bounded.

In this case, if the initial pulse is

$$A(z=0,t)=\begin{cases} A\cos(\pi t/\theta) & |t|<\theta/2 \\ 0 & |t|\geq\theta/2 \end{cases}, \qquad (37)$$

Preprints (www.preprints.org) | NOT PEER-REVIEWED | Posted: 20 January 2019 doi:10.20944/preprints201901.0191.v1

Peer-reviewed version available at Appl. Sci. 2019, 9, 527; doi:10.3390/app9030527

298 which can be rewritten as

299 $$A(z=0,t)=\frac{A}{2}\left\{\left[\exp\left(i\frac{\pi}{\theta}t\right)+\exp\left(-i\frac{\pi}{\theta}t\right)\right]u(-t+\theta/2)-\left[\exp\left(i\frac{\pi}{\theta}t\right)+\exp\left(-i\frac{\pi}{\theta}t\right)\right]u(-t-\theta/2)\right\}, \quad (38)$$

300 then, using (24) the pulse profile at the medium's end is

301 $$A(z,t)=\frac{A_0}{4}\exp\left(i\frac{\beta_2 z}{2}\left(\frac{\pi}{T}\right)^2\right)\left[\exp\left(i\pi\frac{t}{T}\right)erfc\left(\frac{t-T/2+\pi\beta_2 z/T}{\sqrt{-2i\beta_2 z}}\right)+\exp\left(-i\pi\frac{t}{T}\right)erfc\left(\frac{t-T/2-\pi\beta_2 z/T}{\sqrt{-2i\beta_2 z}}\right)-\right.$$
$$\left.\exp\left(i\pi\frac{t}{T}\right)erfc\left(\frac{t+T/2+\pi\beta_2 z/T}{\sqrt{-2i\beta_2 z}}\right)-\exp\left(-i\pi\frac{t}{T}\right)erfc\left(\frac{t+T/2-\pi\beta_2 z/T}{\sqrt{-2i\beta_2 z}}\right)\right]$$

302 (39)

303 Fig.12 illustrates the dynamics of the pulse presented by Eq.(39).

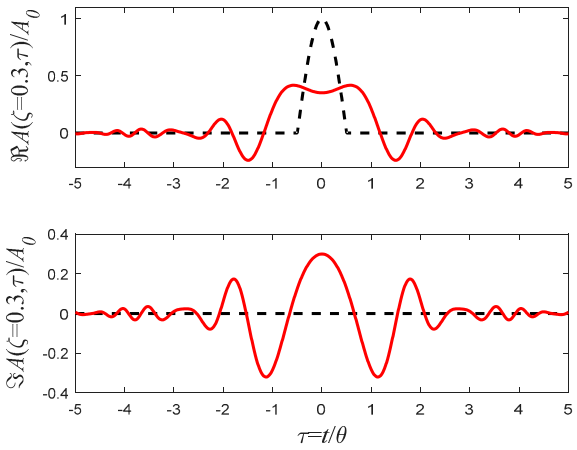

304

305 Fig.12: Similar to Fig.10 but for the bounded cosine pulse [Eq.(39)], and for the final distance of

306 $$\zeta=\beta_2 z/\theta^2=0.3.$$

307 A spatiotemporal presentation of the pulse's intensity is presented in Fig.13.

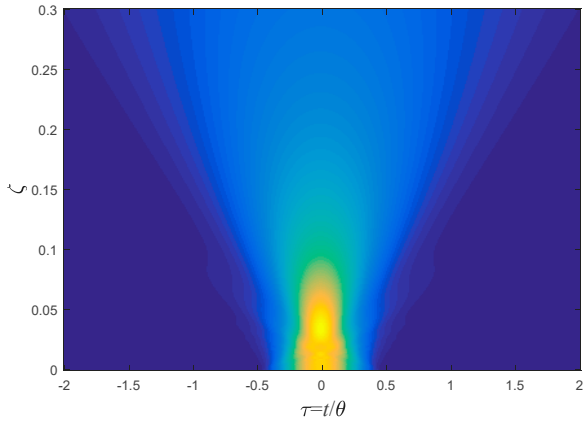

308

309 Fig.13: Same as Fig.2 but for the intensity ($|A(t,z)|^2$) of the pulse presented by Eq.(39).

Preprints (www.preprints.org) | NOT PEER-REVIEWED | Posted: 20 January 2019 doi:10.20944/preprints201901.0191.v1

Peer-reviewed version available at Appl. Sci. 2019, 9, 527; doi:10.3390/app9030527

5.6 Square Cosine Pulse

A smoother pulse profile is the square cosine one. In this case, the discontinuity occurs in the second derivative level, but the function itself and its derivative are both continuous. Therefore, this pulse can simulate pulses, which were generated by discontinuous dielectric media. Let

$$A(z=0,t)=\begin{cases} A_0\cos^2(\pi t/\theta) & |t|<\theta/2 \\ 0 & |t|\geq\theta/2 \end{cases} \tag{40}$$

be the signal's profile at one end of the medium, then, since it can be rewritten as

$$A(z=0,t)=\frac{1}{4}A_0\left[\exp\left(2i\frac{\pi}{\theta}t\right)+\exp\left(-2i\frac{\pi}{\theta}t\right)+2\right]\left[u(-t+\theta/2)-u(-t-\theta/2)\right] \tag{41}$$

Its dynamics can be derived, again using (24), to yield the result

$$A(t,z)=\frac{1}{4}A_0\left[erfc\left(\frac{t-T/2}{\sqrt{-2i\beta_2 z}}\right)-erfc\left(\frac{t+T/2}{\sqrt{-2i\beta_2 z}}\right)\right.$$
$$\exp\left(i\frac{\beta_2 z}{2}\left(\frac{2\pi}{T}\right)^2\right)\left[\exp\left(i2\pi\frac{t}{T}\right)erfc\left(\frac{t-T/2+2\pi\beta_2 z/T}{\sqrt{-2i\beta_2 z}}\right)+\exp\left(-i2\pi\frac{t}{T}\right)erfc\left(\frac{t-T/2-2\pi\beta_2 z/T}{\sqrt{-2i\beta_2 z}}\right)-\right.$$
$$\left.\left.\exp\left(i\pi\frac{t}{T}\right)erfc\left(\frac{t+T/2+\pi\beta_2 z/T}{\sqrt{-2i\beta_2 z}}\right)-\exp\left(-i\pi\frac{t}{T}\right)erfc\left(\frac{t+T/2-\pi\beta_2 z/T}{\sqrt{-2i\beta_2 z}}\right)\right]\right] \tag{42}$$

Fig.14 presents the dynamics of the square cosine pulse.

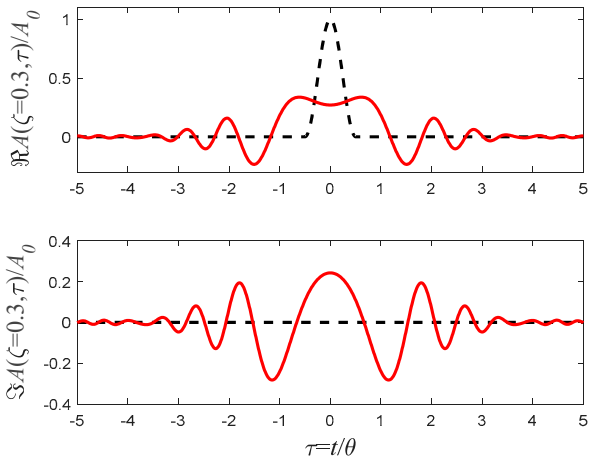

Fig.14: Similar to Fig.12 but for the square cosine pulse[Eq.(42)].

Preprints (www.preprints.org) | NOT PEER-REVIEWED | Posted: 20 January 2019 doi:10.20944/preprints201901.0191.v1

Peer-reviewed version available at Appl. Sci. 2019, 9, 527; doi:10.3390/app9030527

A comparison between (27), (39) and (42) is presented in Fig.15. The three pulses represents three levels of singularities. Eq.(27) represents a case of amplitude discontinuity, Eq.(39) represents discontinuity in the pulse's amplitude's *derivative*, and Eq.(42) represents discontinuity in the amplitude's *second* derivative.

As can clearly be seen, the higher is the level of the singularity (i.e., the discontinuity occurs at higher derivatives) the faster the pulse decays in accordance with Refs.[22] and [23].

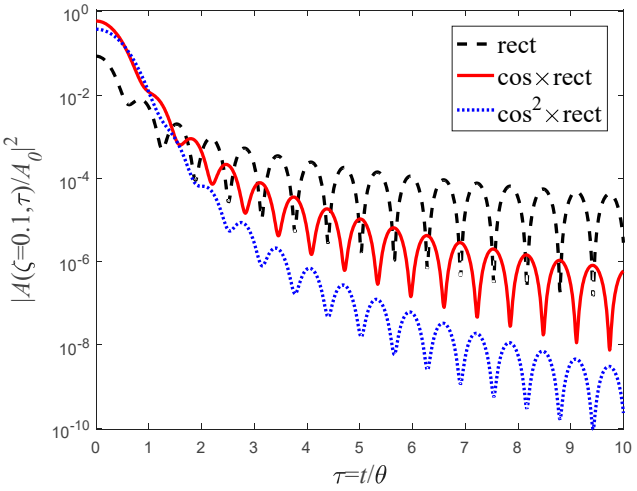

Fig.15: Comparison between the intensities of the three singular pulses Eq.(27)- dashed curve, Eq.(39)-solid curve, and Eq.(42)-dotted curve in a logarithmic scale.

5.7 Generalization and Applicable Examples

The mathematical tools that were presented in the previous sections can be implemented in numerous practical examples. In what follows we will present some examples.

1st example:

Generalization to any power of the bounded cosine pulse, i.e.

$$A(z=0,t)=\begin{cases} A_0\cos^n(\pi t/T) & |t|<T/2 \\ 0 & |t|\geq T/2 \end{cases} \quad \text{for any } n \tag{43}$$

which can be written as

$$A(z=0,t)=\frac{1}{2^n}A_0\left[\exp\left(i\frac{\pi}{T}t\right)+\exp\left(-i\frac{\pi}{T}t\right)\right]^n\left[u(-t+T/2)-u(-t-T/2)\right] \tag{44}$$

and since the brackets can be expanded

$$A(z=0,t)=\frac{1}{2^n}A_0\sum_{k=0}^{n}\binom{n}{k}\exp\left[i(2k-n)\frac{\pi}{T}t\right]\left[u(-t+T/2)-u(-t-T/2)\right] \tag{45}$$

then, using (24) the pulse's profile at the end of the medium is

Preprints (www.preprints.org) | NOT PEER-REVIEWED | Posted: 20 January 2019 doi:10.20944/preprints201901.0191.v1

Peer-reviewed version available at Appl. Sci. 2019, 9, 527; doi:10.3390/app9030527

$$A(z=0,t)=\frac{1}{2^n}A_0\times\sum_{k=0}^{n}\binom{n}{k}\exp\left(i\frac{\beta_2 z}{2}\left(\frac{2\pi}{T}\right)^2\right)\times$$
$$\left[\exp\left(i(2k-n)\pi\frac{t}{T}\right)erfc\left(\frac{t-T/2+(2k-n)\pi\beta_2 z/T}{\sqrt{-2i\beta_2 z}}\right)-\right.$$
$$\left.\exp\left(-i(2k-n)\pi\frac{t}{T}\right)erfc\left(\frac{t-T/2-(2k-n)2\pi\beta_2 z/T}{\sqrt{-2i\beta_2 z}}\right)\right] \quad (46)$$

2nd example:

The initial singular pulse

$$A(z=0,t)=A_0\exp(-a|t|) \quad (47)$$

consists of two exponential pulses, and therefore its propagation can be expressed in a relatively simple form, namely

$$A(z>0,t)=\frac{A_0}{2}\exp\left(-i\frac{\beta_2}{2}a^2 z\right)\left\{\exp(at)erfc\left(\frac{t-i\beta_2 az}{\sqrt{-2i\beta_2 z}}\right)+\exp(-at)erfc\left(\frac{-t-i\beta_2 az}{\sqrt{-2i\beta_2 z}}\right)\right\}. \quad (48)$$

3rd example:

In the previous example, we sew two singular pulses; in general, however, one can sew several pulses together to create a combined pulse, which is much smoother than its singular components. For example, take the following pulse profile

$$A(z=0,t)=\begin{cases}A_0\cos(kt) & |t|<T/2\\ A_0\cos(kT/2)\exp\left[-k\left(|t|-T/2\right)\tan(kT/2)\right] & |t|\geq T/2\end{cases} \quad (49)$$

which consist of three singular and discontinuous pulses; however, the combined pulse and its derivative are both continuous. The discontinuity occurs only in the second derivative. In this case the pulse's amplitude profile obeys

$$A(z,t)=\frac{A_0}{4}\exp\left(i\frac{\beta_2 z}{2}k^2\right)\left[\exp(ikt)erfc\left(\frac{t-T/2+k\beta_2 z}{\sqrt{-2i\beta_2 z}}\right)+\exp(-ikt)erfc\left(\frac{t-T/2-k\beta_2 z}{\sqrt{-2i\beta_2 z}}\right)-\right.$$
$$\left.\exp(ikt)erfc\left(\frac{t+T/2+k\beta_2 z}{\sqrt{-2i\beta_2 z}}\right)-\exp(-ikt)erfc\left(\frac{t+T/2-k\beta_2 z}{\sqrt{-2i\beta_2 z}}\right)\right]+$$
$$\frac{1}{2}A_0\cos(kT/2)\exp\left(-i\frac{\beta_2}{2}(k\tan(kT/2))^2 z\right)\times \quad (50)$$
$$\left[\exp(k\tan(kT/2)t)erfc\left(\frac{t-T/2-i\beta_2 k\tan(kT/2)z}{\sqrt{-2i\beta_2 z}}\right)\right.$$
$$\left.\exp(-k\tan(kT/2)t)erfc\left(\frac{-t-T/2-i\beta_2 k\tan(kT/2)z}{\sqrt{-2i\beta_2 z}}\right)\right]$$

Preprints (www.preprints.org) | NOT PEER-REVIEWED | Posted: 20 January 2019 doi:10.20944/preprints201901.0191.v1

Peer-reviewed version available at Appl. Sci. 2019, 9, 527; doi:10.3390/app9030527

4th example:

The discontinuity of the exponential pulse can be reduced by multiplying the pulse by a sine function, i.e.,

$$A(z=0,t)=-A_0\exp(at)\sin(bt)u(-t). \tag{51}$$

Since the pulse can be written as

$$A(z=0,t)=\frac{iA_0}{2}\left[\exp((a+ib)t)-\exp((a-ib)t)\right]u(-t) \tag{52}$$

then the pulse's amplitude after a distance z reads

$$A(t,z)=\frac{iA_0}{4}\exp\left(-i\frac{\beta_2}{2}\left(a^2-b^2\right)z+at\right)\times \left[\exp(\beta_2 abz+ibt)erfc\left(\frac{t-i\beta_2 z(a+ib)}{\sqrt{-2i\beta_2 z}}\right)-\exp(-\beta_2 abz-ibt)erfc\left(\frac{t-i\beta_2 z(a-ib)}{\sqrt{-2i\beta_2 z}}\right)\right] \tag{53}$$

In Fig.16 this pulse is presented for two cases with different parameters. On the right figure the frequency is equal to the decaying coefficient a, however, on the left one the frequency is higher than the decaying exponent a, and therefore the profile initially oscillates.

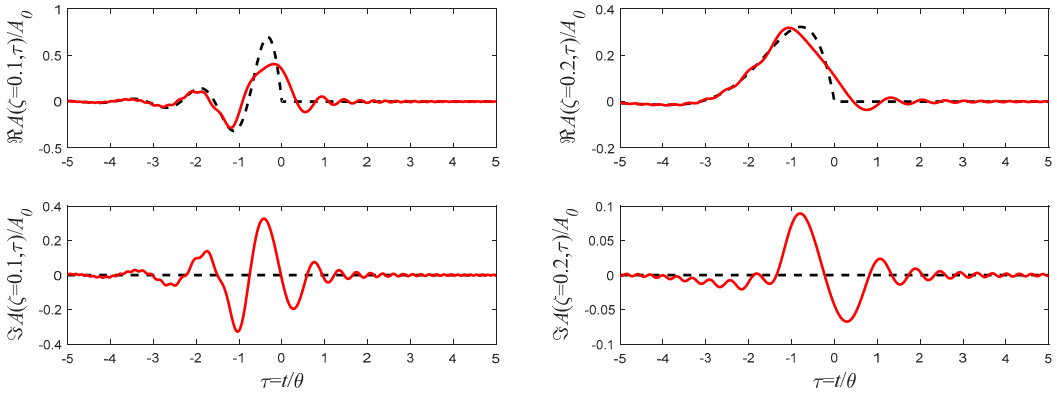

Fig.16: Similar to Fig.10 but for the pulse presented by Eq.(53). In these plots, $a=1/\theta$ on both, but $b=4/\theta$ on the left figure (final distance corresponds to $\zeta=\beta_2 z/\theta^2=0.1$) and $b=1/\theta$ on the right one (final distance corresponds to $\zeta=\beta_2 z/\theta^2=0.2$).

6. Smooth Pulses

Thus far, we have analyzed, except for the Gaussian pulses, only singular pulses, i.e., pulses' profiles, which have at least one singularity point. Most of them can simulate real physical pulses' profiles; however, one may argue that these pulses fundamentally cannot behave like physical pulses. In some respects, it is indeed a justified claim, especially for short medium. It has been shown that since the dispersion equation is not a causal equation, any singularity has a nonlocal effects, which do not exist in real pulses [19,20,22,24]. However, it

Preprints (www.preprints.org) | NOT PEER-REVIEWED | Posted: 20 January 2019 doi:10.20944/preprints201901.0191.v1

Peer-reviewed version available at Appl. Sci. 2019, 9, 527; doi:10.3390/app9030527

comes out that there is a very elegant method, to convert each one of these singular pulses to a smooth one, which can simulate, in all respect, a real physical profile pulse. This method was first presented in Refs. [23] and [24] for the rectangular pulse.

6.1 Smooth Step Function

In principle, any smooth step function can replace the Heaviside step function, however, there is a clear advantage to choose the complementary error function for that purpose. The function

$$\frac{1}{2}erfc\left(\frac{t}{\Delta}\right) \tag{54}$$

is an approximation of the step function in the sense that

$$\lim_{|t/\Delta|\to\infty}\frac{1}{2}erfc\left(\frac{t}{\Delta}\right)=u(-t) \tag{55}$$

However, unlike the step function, the transition in (54) occurs within the time scale Δ.

Equivalently, a step function signal that passes through a Gaussian low-pass filter, whose spectral FWHM is δ will have the following form [11]

$$\frac{1}{2}erfc\left(\pi\delta\frac{t}{\sqrt{2\ln 2}}\right). \tag{56}$$

Therefore, the relation between the transition time scale Δ and the spectral FWHM δ is

$$\delta=\sqrt{2\ln(2)}\theta/\pi\Delta. \tag{57}$$

Moreover, and this is the reason that (54) is very useful in replacing step functions, the smooth step (54) can be written as a convolution between the step function and a Gaussian, i.e.

$$\frac{1}{2}erfc\left(\frac{t}{\Delta}\right)=\frac{1}{\sqrt{\pi}}\int_{t/\Delta}^{\infty}\exp\left(-x^2\right)dx=\frac{1}{\Delta\sqrt{\pi}}\int_{-\infty}^{\infty}u(\tau-t)\exp\left(-\tau^2/\Delta^2\right)d\tau= u(-t)*\frac{1}{\Delta\sqrt{\pi}}\exp\left(-t^2/\Delta^2\right) \tag{58}$$

where the asterisk represents temporal convolution. However, since the effect of dispersion can also be represented as a convolution with the kernel (4), then the propagation of the initial pulse' profile

$$A(t,0)=\frac{A_0}{2}erfc\left(\frac{t}{\Delta}\right) \tag{59}$$

can be written simply as

$$A(t,0)=A_0u(-t)*\frac{1}{\Delta\sqrt{\pi}}\exp\left(-t^2/\Delta^2\right)*K(t,z)=\frac{1}{2}A_0erfc\left(\frac{t}{\sqrt{\Delta^2-2i\beta_2z}}\right) \tag{60}$$

Therefore, *every* step function from the previous section can be replaced with the smooth step function. In particular, the boosted smooth step function

Preprints (www.preprints.org) | NOT PEER-REVIEWED | Posted: 20 January 2019 doi:10.20944/preprints201901.0191.v1

Peer-reviewed version available at Appl. Sci. 2019, 9, 527; doi:10.3390/app9030527

$$A(z=0,t)=\frac{A}{2}\exp(-i\omega_0 t)erfc\left(\frac{t}{\Delta}\right) \tag{61}$$

will have the following profile at the end of the medium

$$A(z>0,t)=\frac{A}{2}\exp\left(i\frac{\beta_2}{2}\omega_0^2 z-i\omega_0 t\right)erfc\left(\frac{t-\beta_2\omega_0 z}{\sqrt{\Delta^2-2i\beta_2 z}}\right) \tag{62}$$

Sample Applications: The rise time of pulses in optical communications are usually defined as the time-period it takes to rise from 10% to 90% maximum intensity value. Therefore, provided this rise-time (Δt_{10-90}) is given then Δ can be derived by $\Delta\cong 0.67\Delta t_{10-90}$. If the rise time is defined as the period, in which the signal rises from 25% to 75% of its maximum intensity value (Δt_{25-75}), then $\Delta\cong 1.28\Delta t_{25-75}$.

6.2 Smooth Rectangular Pulse

Similarly, the smooth rectangular pulse

$$A(z=0,t)=\frac{A_0}{2}\left[erfc\left(\frac{t-\theta/2}{\Delta}\right)-erfc\left(\frac{t+\theta/2}{\Delta}\right)\right] \tag{63}$$

will appear at the end of the medium in the following form

$$A(z>0,t)=A_0\,\mathrm{srect}_1\left(\frac{t}{\theta},\sqrt{2\ln(2)}\frac{\theta}{\pi\Delta},\frac{\beta_2 z}{\theta^2}\right)=\frac{A_0}{2}\left[erfc\left(\frac{t-\theta/2}{\sqrt{-2i\beta_2 z+\Delta^2}}\right)-erfc\left(\frac{t+\theta/2}{\sqrt{-2i\beta_2 z+\Delta^2}}\right)\right] \tag{64}$$

where

$$\mathrm{srect}_\xi(\tau,\delta,\zeta)\equiv\left\{\mathrm{erfc}\left[(\tau-\xi/2)/\sqrt{i2\zeta+2\ln(2)/\pi^2\delta^2}\right]-\mathrm{erfc}\left[(\tau+\xi/2)/\sqrt{i2\zeta+2\ln(2)/\pi^2\delta^2}\right]\right\}/2 \tag{65}$$

is the smooth rectangular function (see Refs.[23-25]), which describes the dispersion dynamics of a smooth rectangular pulse.

In Fig. 17 this smooth rectangular pulse's profile is presented for the same values as in Fig.6, i.e. the perfect rectangular pulse. However, the difference is that in Fig.17 the pulse's boundaries are smooth instead of discontinuous. As can be seen, due to the smooth transition, the oscillations, which appear in Fig.6 disappear in Fig.17.

Preprints (www.preprints.org) | NOT PEER-REVIEWED | Posted: 20 January 2019 doi:10.20944/preprints201901.0191.v1

Peer-reviewed version available at Appl. Sci. 2019, 9, 527; doi:10.3390/app9030527

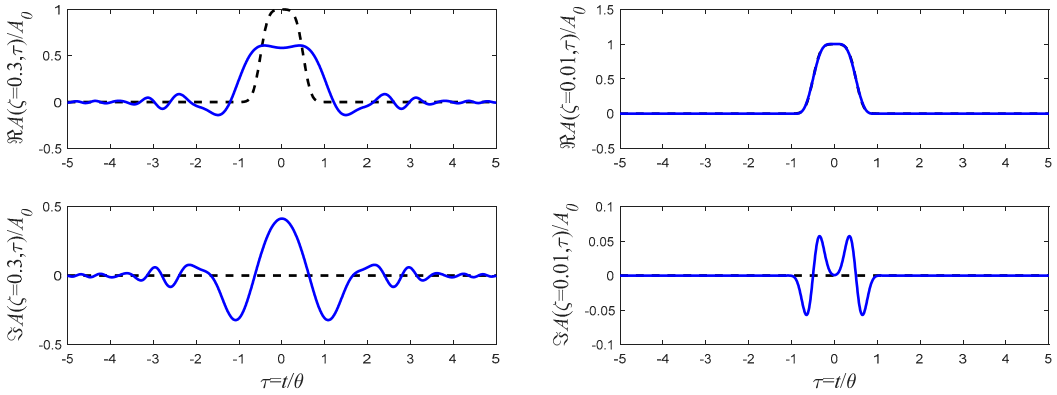

Fig.17: Same as Fig.12, but for Eq.(64) with the transition width $\Delta = 0.2\theta$

This pulse has numerous applications in optical communications.

For example, if the transmitted data is encoded in the amplitudes of these smooth rectangular pulses, then the transmitted signal profile can be written

$$A(t, z>0) = \sum_n a_n \,\mathrm{srect}_\xi\left(t/\theta - n, \sqrt{2\ln(2)}\frac{\theta}{\pi\Delta}, \beta_2 z/\theta^2 \right). \tag{66}$$

where a_n are coefficient, which carry the data.

These pulses has two properties that make them especially suitable for stream of pulses.

The ξ parameter can determine the signal's protocol. The Return-to-Zero (RZ) protocol occurs for $\xi < 1$, when ξ determines the duty cycle. However, when $\xi = 1$ then this is a perfect Non-Return-to-Zero (NRZ) protocol. The second property, which is more important, emerges due to symmetry of the erfc function. Since

$$erfc\left(\frac{t}{\Delta}\right) + erfc\left(\frac{-t}{\Delta}\right) = 2 \tag{67}$$

then two adjacent smooth rectangular pulses look exactly like a single but twice as wide a pulse, i.e.

$$\mathrm{srect}_1(\tau - 0.5, \delta, \zeta) + \mathrm{srect}_1(\tau + 0.5, \delta, \zeta) = \mathrm{srect}_2(\tau, \delta, \zeta) \tag{68}$$

Sample Application: In 40Gb/s optical communications channel (over smf28 fiber) with a carrier wavelength of $\lambda = 1.55\mu m$, the pulses can be simulated by rectangular ones with $\theta = 25ps$, $\beta_2 \cong 20ps^2/Km$, in which case $\zeta = 0.3$ and $\zeta = 0.01$ in Fig.17 correspond to $z = \zeta\theta^2/\beta_2 \cong 9.4Km$, and $z \cong 0.31Km$ respectively. Since $\Delta = 0.2\theta$ then the 10%-90% rise time correspond to $\Delta t_{10-90} \cong \Delta/0.67 = 0.2\theta/0.67 \cong 7.5ps$.

6.3 Relations to Super-Gaussian Pulses

The smooth rectangular pulses can be an excellent approximation for super-Gaussian ones. Let

Preprints (www.preprints.org) | NOT PEER-REVIEWED | Posted: 20 January 2019 doi:10.20944/preprints201901.0191.v1

Peer-reviewed version available at Appl. Sci. 2019, 9, 527; doi:10.3390/app9030527

$$A(z=0,t)=A_0\exp\left[-(t/T)^n\right] \tag{69}$$

be a super-Gaussian pulse. This pulse can be approximated by a smooth rectangular one (Eq.(63)] $A(z=0,t)=A_0\left[erfc((t-\theta/2)/\Delta)-erfc((t+\theta/2)/\Delta)\right]/2$ by choosing the following parameters

$$\theta=2T(\ln 2)^{1/n} \tag{70}$$

and

$$\Delta=\frac{2T}{\sqrt{\pi}n(\ln 2)^{(n-1)/n}} \tag{71}$$

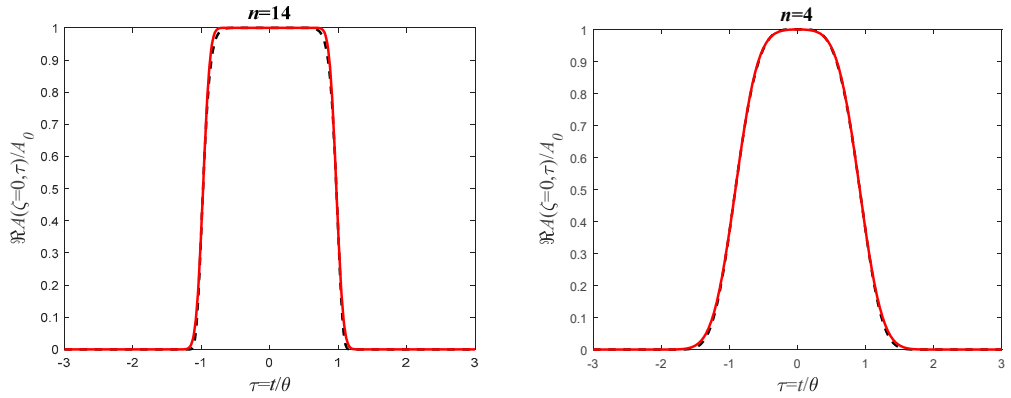

Fig.18: A comparison between smooth rectangular pulses Eq.(63) (solid curves) and super-gaussian pulses Eq.(69) (dashed curves) for $n=4$ (right) and $n=14$ (left). In these plots only the real part of the fields is presented. The imaginary part is zero.

In Fig.18 such a comparison is presented for two different values of the super Gaussian order n. This figure clearly shows that the smooth rectangular is an excellent approximation to super-Gaussian, while unlike super-Gaussian, the smooth rectangular pulse does have an exact analytical expression for its propagation in dispersive medium.

6.4 Chirped Smooth Rectangular Pulse

The case of the chirped rectangular pulse can be generalized to the chirped smooth rectangular one. That is, if the initial pulse's profile is

$$A(z=0,t)=\frac{A_0}{2}\exp\left(-iq^2t\right)\left[erfc\left(\frac{t-\theta/2}{\Delta}\right)-erfc\left(\frac{t+\theta/2}{\Delta}\right)\right] \tag{72}$$

Then, after a certain distance in the dispersive medium, the pulse's profile will be

Preprints (www.preprints.org) | NOT PEER-REVIEWED | Posted: 20 January 2019 doi:10.20944/preprints201901.0191.v1

Peer-reviewed version available at Appl. Sci. 2019, 9, 527; doi:10.3390/app9030527

$$A(z>0,t)=(1+2\beta_2 zq)^{-1/2}\exp\left(-i\frac{t^2}{2\beta_2 z+1/q}\right)\frac{A_0}{2}\left[erfc\left(\frac{\frac{t}{1+2\beta_2 zq}-\theta/2}{\sqrt{\frac{-2i\beta_2 z}{1+2\beta_2 zq}+\Delta^2}}\right)-erfc\left(\frac{\frac{t}{1+2\beta_2 zq}+\theta/2}{\sqrt{\frac{-2i\beta_2 z}{1+2\beta_2 zq}+\Delta^2}}\right)\right] \quad (73)$$

A spatiotemporal presentation of the pulse's intensity is presented in Fig.18. The fact that the initial pulse is smooth eliminates the ripples that appear in Fig.9.

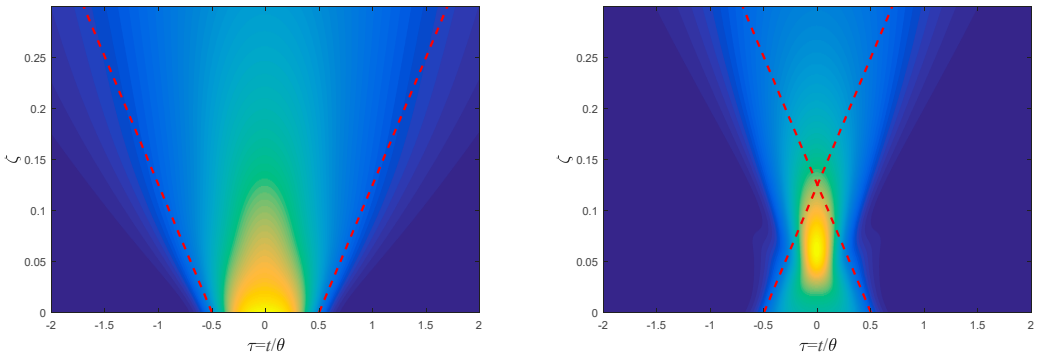

Fig.18: Same as Fig.8 but for a smooth rectangular pulse with $\Delta=0.25\theta$.

6.5 Smooth Cosine Pulse

As was said above, the same procedure can be applied to every singular pulse, i.e., to replace the singular step function with the erfc functions. For example, the singular cosine pulse (37) can be replaced with the following smooth cosine one

$$A(z=0,t)=A_0\cos\left(\frac{\pi}{\theta}t\right)\left[erfc\left(\frac{t-\theta/2}{\Delta}\right)-erfc\left(\frac{t+\theta/2}{\Delta}\right)\right] \quad (74)$$

which has the following solution for any distance z:

$$A(z,t)=\frac{A_0}{4}\exp\left(i\frac{\beta_2 z}{2}\left(\frac{\pi}{\theta}\right)^2\right)\left[\exp\left(i\pi\frac{t}{\theta}\right)erfc\left(\frac{t-\theta/2+\pi\beta_2 z/\theta}{\sqrt{\Delta^2-2i\beta_2 z}}\right)+\exp\left(-i\pi\frac{t}{\theta}\right)erfc\left(\frac{t-\theta/2-\pi\beta_2 z/\theta}{\sqrt{\Delta^2-2i\beta_2 z}}\right)-\exp\left(i\pi\frac{t}{\theta}\right)erfc\left(\frac{t+\theta/2+\pi\beta_2 z/\theta}{\sqrt{\Delta^2-2i\beta_2 z}}\right)-\exp\left(-i\pi\frac{t}{\theta}\right)erfc\left(\frac{t+\theta/2-\pi\beta_2 z/\theta}{\sqrt{\Delta^2-2i\beta_2 z}}\right)\right] \quad (75)$$

Clearly, when $\Delta\to 0$ Eq.(75) converges to Eq.(39). In Fig.19 the amplitude profile of Eq.75 is presented.

Preprints (www.preprints.org) | NOT PEER-REVIEWED | Posted: 20 January 2019 doi:10.20944/preprints201901.0191.v1

Peer-reviewed version available at Appl. Sci. 2019, 9, 527; doi:10.3390/app9030527

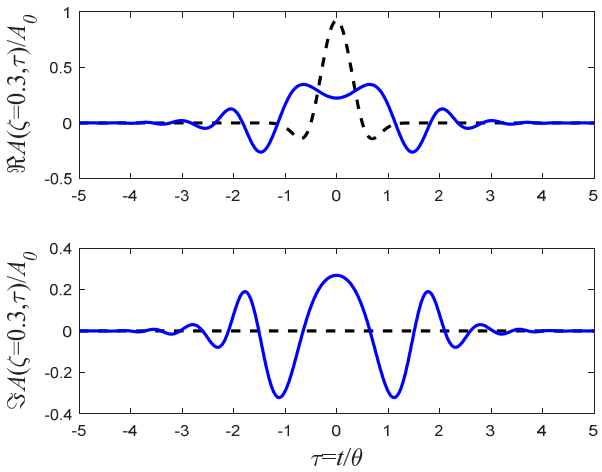

Fig.19: Same as Fig.12, but for Eq.(75) with the transition width $\Delta = 0.4\theta$

Clearly, the same procedure can be implemented on the square cosine pulse or on any other singular pulse from the previous sections.

6.6 Smooth Exponential Pulse

By following the same procedure, one can replace the singular exponential with the following smooth exponential pulse

$$A(z=0,t)=\frac{1}{2}A_0\exp(at)erfc\left(\frac{t}{\Delta}\right) \tag{76}$$

which propagates in dispersive medium according to

$$A(z>0,t)=\frac{A_0}{2}\exp\left(-i\frac{\beta_2}{2}a^2z+at\right)erfc\left(\frac{t-i\beta_2 az}{\sqrt{\Delta^2-2i\beta_2 z}}\right) \tag{77}$$

This function is illustrated in Fig.20 for two different distances.

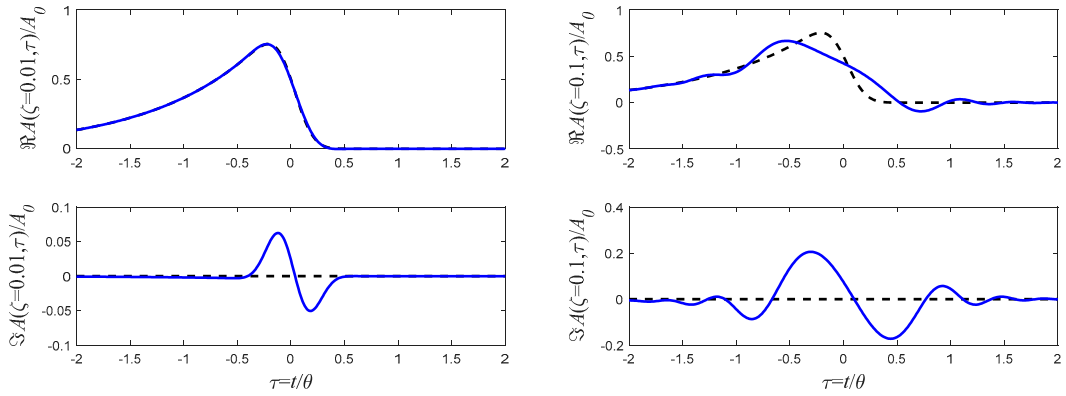

Fig.20: Same as Fig.10, but for Eq.(77) with the transition width $a=1/\theta$ and $\Delta=0.2\theta$, for two final distances $\zeta=\beta_2 z/\theta^2=0.01$ on the left and $\zeta=\beta_2 z/\theta^2=0.1$ on the right.

Preprints (www.preprints.org) | NOT PEER-REVIEWED | Posted: 20 January 2019 doi:10.20944/preprints201901.0191.v1

Peer-reviewed version available at Appl. Sci. 2019, 9, 527; doi:10.3390/app9030527

Sample Application: A pulse with a 10% to 90% rise time of $\Delta t_{10-90} = 1ps$ and a decay time of ~3.7ps with a carrier wavelength of $\lambda = 2.0\mu m$, can be simulated by the pulse presented by Eq.(76) with $\Delta = 0.67ps$, $a = 0.3ps^{-1}$. Since $a\Delta \cong 0.2$, Fig.20 is an illustration of this pulse. If the pulse penetrates a BK7 glass then for this wavelength $\beta_2 \cong 98ps^2/Km$, and therefore $\zeta = 0.1$ and $\zeta = 0.01$ in the figure correspond to $z = \zeta\theta^2/\beta_2 \cong 11m$, and $z \cong 1.1m$ respectively.

7. Singular Pulses in the Spectral Domain

7.1 The ideal Nyquist Sinc Pulse

One of the interesting and important pulses, which belongs to this category and received a lot of attention recently in the literature, is the Nyquist-Sinc pulse (see, for example, Refs.[26-31]).

These pulses are useful in optical communications for several reasons, one of which is that they are resilient against chromatic dispersion. Moreover, these pulses, like their Fourier counterpart – the rectangular pulses, are orthogonal both in the time and in the frequency domains.

The initial Nyquist-Sinc pulse is singular in the spectral domain, i.e. its Fourier transform is

$$A(z=0,\omega) = \theta A_0 rect_1(\omega\theta/2\pi) . \tag{78}$$

In the temporal regime the "sinc" profile appears

$$A(z=0,t) = A_0 \operatorname{sinc}\left(\frac{t}{\theta}\right) \equiv A_0 \frac{\sin(\pi t/\theta)}{\pi t/\theta}. \tag{79}$$

Since the pulse's spectrum has a simple rectangular shape, the temporal dynamics is straightforward, namely

$$A(z,t) = A_0\,\mathrm{dsinc}(\tau,\zeta) \equiv \frac{A_0}{2}\sqrt{\frac{i\theta^2}{2\pi\beta_2 z}}\exp\left(-i\frac{t^2}{2\beta_2 z}\right)\left[\operatorname{erf}\left(-\frac{t-|\pi\beta_2 z/\theta|}{\sqrt{i2\beta_2 z}}\right)-\operatorname{erf}\left(-\frac{t+|\pi\beta_2 z/\theta|}{\sqrt{i2\beta_2 z}}\right)\right] \tag{80}$$

where

$$\mathrm{dsinc}(\tau,\zeta) \equiv \frac{1}{2}\sqrt{\frac{i}{2\pi\zeta}}\exp\left(-i\frac{\tau^2}{2\zeta}\right)\left[\operatorname{erf}\left(-\frac{\tau-\pi|\zeta|}{\sqrt{i2\zeta}}\right)-\operatorname{erf}\left(-\frac{\tau+\pi|\zeta|}{\sqrt{i2\zeta}}\right)\right] \tag{81}$$

is the "dynamic" sinc function[12]. Clearly $\mathrm{dsinc}(\tau,\zeta=0) = \operatorname{sinc}(\tau) \equiv \frac{\sin(\pi\tau)}{\pi\tau}$.

In Fig.21 the amplitude profile of this pulse is presented.

Preprints (www.preprints.org) | NOT PEER-REVIEWED | Posted: 20 January 2019 doi:10.20944/preprints201901.0191.v1

Peer-reviewed version available at Appl. Sci. 2019, 9, 527; doi:10.3390/app9030527

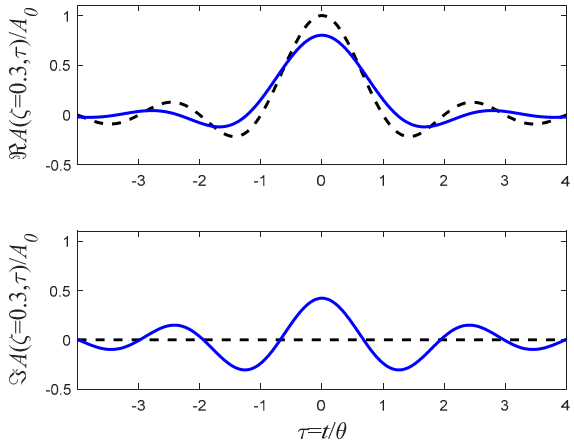

Fig.21: Same as Fig.10, but for Eq.(80) and for the final distance of $\zeta = \beta_2 z / \theta^2 = 0.3$

The spatiotemporal presentation of the pulse's intensity is presented in Fig.22.

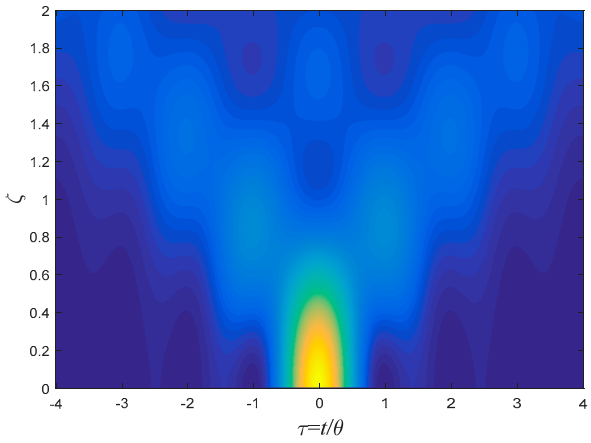

Fig.22: Same as Fig.2 but for the intensity ($|A(t,z)|^2$) of the pulse presented by Eq.(80).

7.2 Nyquist Sinc Pulse with Smooth Spectrum

Singular spectrum may simulate real pulses, but in real scenarios, singularities can neither occur in the spectral domain. We can therefore utilize the theorems and conclusions from the previous sections to smooth spectrally the Nyquist-Sinc pulse.

Thus, the singular rectangular spectrum of the Nyquist-Sinc pulse, i.e.,

$$A(z=0,\omega)=\theta A_0 rect_1(\omega\theta/2\pi) \tag{82}$$

can be replaced with its smooth counterpart

$$A(z=0,\omega)=\theta A_0 \frac{1}{2}\left[erfc\left(\frac{\omega-\pi/\theta}{\Delta}\right)-erfc\left(\frac{\omega+\pi/\theta}{\Delta}\right)\right]. \tag{83}$$

Preprints (www.preprints.org) | NOT PEER-REVIEWED | Posted: 20 January 2019 doi:10.20944/preprints201901.0191.v1

Peer-reviewed version available at Appl. Sci. 2019, 9, 527; doi:10.3390/app9030527

548 However, this expression can be written as a convolution is the spectral domain, i.e.,

549 $$A(z=0,\omega)=\theta A_0 rect_1(\omega\theta/2\pi)*\frac{1}{\Delta\sqrt{\pi}}\exp\left[-(\omega/\delta)^2\right] \quad (84)$$

550 and therefore the initial pulse profile can be written as a product of a sinc function and a Gaussian one, i.e.,

551 $$A(z=0,t)=A_0\frac{\sin(\pi t/\theta)}{\pi t/\theta}\frac{1}{2\pi}\exp\left[-(t\delta/2)^2\right]. \quad (85)$$

552 Using (12) and (80) we finally obtain

553 $$A(t,z)=\frac{A_0}{2}\exp\left(-i\frac{t^2}{2\beta_2 z}\right)\sqrt{\frac{i\theta^2}{2\pi\beta_2 z}}\left[\mathrm{erf}\left(-\frac{t-|\pi\beta_2 z/\theta|}{\sqrt{i2\beta_2 z(1-i\beta_2 z\delta^2/2)}}\right)-\mathrm{erf}\left(-\frac{t+|\pi\beta_2 z/\theta|}{\sqrt{i2\beta_2 z(1-i\beta_2 z\delta^2/2)}}\right)\right] \quad (86)$$

554 In Fig.23 the amplitude of Eq.(86) is plotted. Unlike ordinary Nyquist-Since pulses, this pulse decays
555 exponentially.

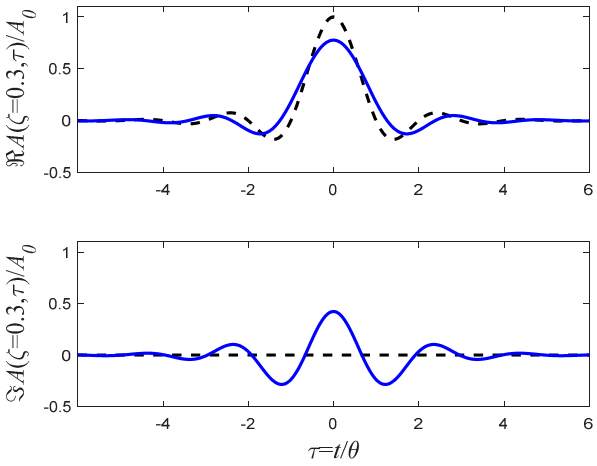

556

557 Fig.23: Same as Fig.21, but for Eq.(86) with $\delta=0.6/\theta$.

558

559 **8. Undistorted Airy Pulses**

560 *8.1 Undistorted Ideal Accelerating Pulses*

561 One of the interesting properties of the Schrödinger equation in general and the dispersion equation in
562 particular, is that the Airy function is its accelerating solution[32-34]. However, despite dispersion, the shape of
563 this accelerating solution remains intact during propagation. This property can be useful in optical
564 communications, where the encoded data propagates in the dispersive medium without experiencing
565 distortions.

566 That is, if the initial pulse is an Airy function pulse

567 $$A(t,z)=A_0\,\mathrm{Ai}(t/\theta) \quad (87)$$

568 where $\mathrm{Ai}(\tau)$ stands for the Airy function [35], then the pulse at the end of the dispersive medium keeps its
569 initial profile, despite being accelerated, i.e., after a distance z, it reads

Preprints (www.preprints.org) | NOT PEER-REVIEWED | Posted: 20 January 2019 doi:10.20944/preprints201901.0191.v1

Peer-reviewed version available at Appl. Sci. 2019, 9, 527; doi:10.3390/app9030527

$$A(t,z)=A_0 Ai\left[t/\theta-\left(\beta_2 z/2\theta^2\right)^2\right]\exp\left[-it\beta_2 z/2\theta^3+i\left(\beta_2 z/\theta^2\right)^3/12\right] \quad (88)$$

In Fig.24 the dynamics of this pulse is presented for different distances.

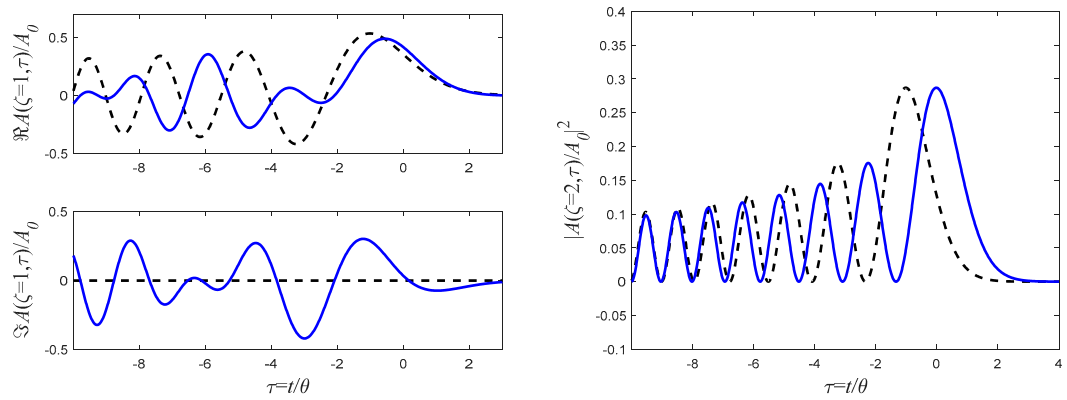

Fig.24: Presentation of the temporal dynamics of the accelerating Airy pulse, Eq.(88). On the left the real and imaginary components of the pulse's field are presented (for the final distance of $\zeta=\beta_2 z/\theta^2=1$), and on the right, the pulse's intensity ($|A(t,z)|^2$) is presented (for the final distance of $\zeta=\beta_2 z/\theta^2=2$).

As can be seen in Fig.24, the shape of the pulse remains intact, while the pulses accelerates according to the equation

$$t=\left(\beta_2 z\right)^2/4\theta^3 \quad (89)$$

i.e., the square of the dispersion coefficient is proportional to the pulse's "acceleration".

8.2 Physical Accelerating Pulse

Clearly, the main problem with the Airy function is that it is not a normalizable function, i.e., it has infinite energy and can have no physical realization.

One option to normalize the airy function is to multiply the pulse by an exponent [36], i.e.

$$A(z=0,t)=A_0\exp(at)\mathrm{Ai}(t/\theta) \quad (90)$$

In which case the pulse dynamics can be derived with the aid of (8) and (88), yielding

$$A(z,t)=A_0 Ai\left[\frac{t-i\beta_2 az}{\theta}-\left(\frac{\beta_2 z}{2\theta^2}\right)^2\right]\exp\left[-i\frac{\beta_2}{2}a^2 z+at-i\frac{\beta_2 z(t-i\beta_2 az)}{2\theta^3}+\frac{i}{12}\left(\frac{\beta_2 z}{\theta^2}\right)^3\right] \quad (91)$$

A spatiotemporal presentation of the pulse's intensity is presented in Fig.26. This pulse has a finite energy (it can be normalized) but as a consequence, the pulse decays in the z-direction as well. Since

Preprints (www.preprints.org) | NOT PEER-REVIEWED | Posted: 20 January 2019 doi:10.20944/preprints201901.0191.v1

Peer-reviewed version available at Appl. Sci. 2019, 9, 527; doi:10.3390/app9030527

591 $$|A(z,t)|^2 = |A_0|^2 \left| Ai\left[\frac{t - i\beta_2 az}{\theta} - \left(\frac{\beta_2 z}{2\theta^2} \right)^2 \right] \right|^2 \exp\left(2at - a\frac{(\beta_2 z)^2}{\theta^3} \right) \quad (92)$$

592

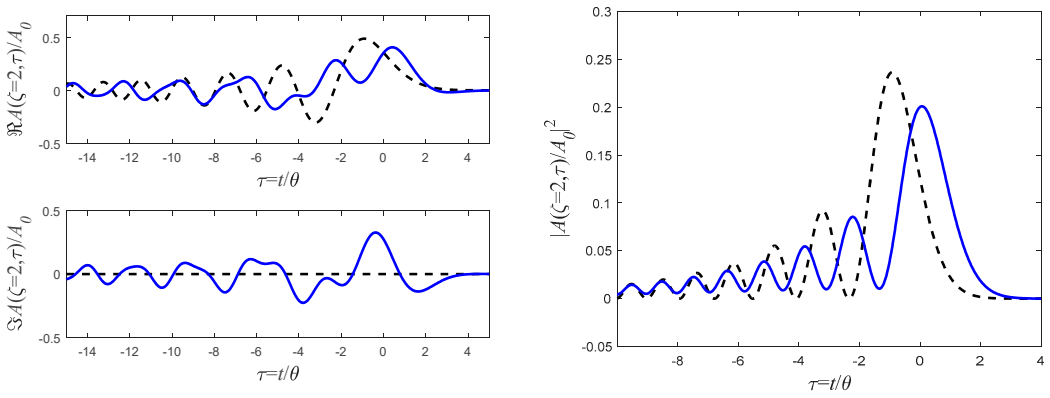

593

594 Fig.25: Same as Fig.24, but for Eq.(90) with $a = 0.1/\theta$ (for the final distance of $\zeta = \beta_2 z/\theta^2 = 2$).

595

596 the pulse's confinement within the time-scale a^{-1} "costs" resultant confinement in the z-direction, i.e., the

597 pulse decays within a distance of $z \cong \sqrt{\theta^3/a}/\beta_2$.

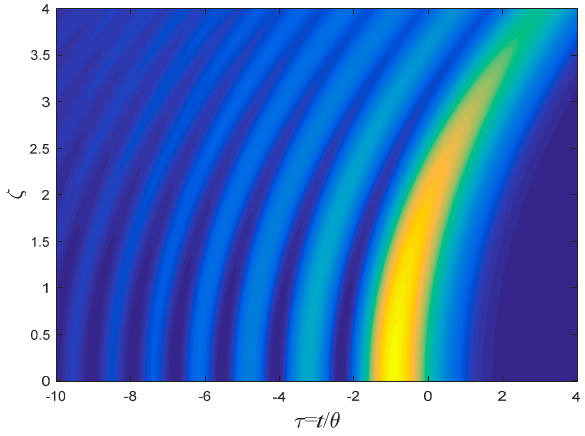

598

599 Fig.26: Same as Fig.2 but for the intensity ($|A(t,z)|^2$) of the pulse presented by Eq.(92).

600 *8.3 Attenuation Compensating Airy pulse*

601 It has been realized that the Airy beams can be implemented to compensate medium's attenuation. Energy can
602 flow from minus infinity to compensate for the pulse's attenuation. Such a pulse can be constructed by
603 imaginary period displacement [37,38], i.e.,

604 $$A(t,z) = A_0 \,\mathrm{Ai}[(t - i\eta)/\theta] \quad (93)$$

605 In this case, the pulse at the end of the dispersive medium can be directly derived

Preprints (www.preprints.org) | NOT PEER-REVIEWED | Posted: 20 January 2019 doi:10.20944/preprints201901.0191.v1

Peer-reviewed version available at Appl. Sci. 2019, 9, 527; doi:10.3390/app9030527

606 $$A(t,z)=A_0\,\mathrm{Ai}\left[(t-i\eta)/\theta-\left(\beta_2 z/2\theta^2\right)^2\right]\exp\left[i(t-i\eta)\beta_2 z/2\theta^3-i\left(\beta_2 z/\theta^2\right)^3/12\right] \quad (94)$$

607 This expression is presented in Fig.27.

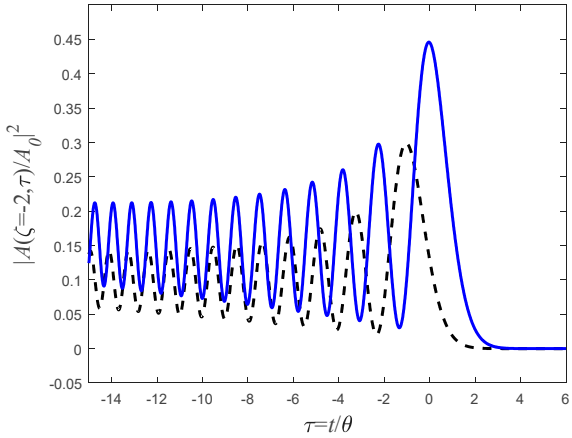

608

609 Fig. 27: Same as the right figure in Fig.24, but with $\eta/\theta=0.2$.

610 The introduction of η is responsible to the additional exponential term $\exp\left[\eta\beta_2 z/2\theta^3\right]$, which can

611 compensate for the medium's absorption.

612 The problem with these pulses is, again, that they have infinite energy and cannot be normalized. Therefore,
613 only approximations of these pulses can be implemented in real experiments (see, for example, Ref.[38]).

614

615 *8.4 Physical Attenuation Compensating Airy pulse*

616 In the previous section we have seen that a complex Airy pulse can compensate pulse attenuation. However,
617 these pulses cannot be normalized. One option to turn these pulses to a finite energy ones, and therefore
618 normalizable, is to multiply them by an exponential function, i.e., to choose the following initial pulse profile

619 $$A(z,t)=A_0\,\mathrm{Ai}\left(\frac{t-i\eta}{\theta}\right)\exp(at) \quad (95)$$

620 then, following (8) and (93), the pulse after a distance z has the following form

621 $$A(z,t)=A_0\,\mathrm{Ai}\left[\frac{t-i\eta+i\beta_2 az}{\theta}-\left(\frac{\beta_2 z}{2\theta^2}\right)^2\right]\exp\left[i\frac{\beta_2}{2}a^2z+at+i\frac{\beta_2 z(t-i\eta+i\beta_2 az)}{2\theta^3}-\frac{i}{12}\left(\frac{\beta_2 z}{\theta^2}\right)^3\right] \quad (96)$$

622 The intensity of this pulse

623 $$|A(z,t)|^2=\left|A_0\,\mathrm{Ai}\left[\frac{t-i\eta+i\beta_2 az}{\theta}-\left(\frac{\beta_2 z}{2\theta^2}\right)^2\right]\right|^2\exp\left[2at-\frac{\beta_2 z(\beta_2 az-\eta)}{\theta^3}\right] \quad (97)$$

624 is presented in Fig.28. One can easily see, that unlike Fig.25 the pulse *increases* in short distances, but unlike
625 Fig. 27, *it has finite energy*, and therefore, unlike Eq.(94), can be implemented in real physical scenarios.

Preprints (www.preprints.org) | NOT PEER-REVIEWED | Posted: 20 January 2019 doi:10.20944/preprints201901.0191.v1

Peer-reviewed version available at Appl. Sci. 2019, 9, 527; doi:10.3390/app9030527

626 Clearly, however, the pulse will eventually decay. It will reach its maximum intensity at $z = \eta/\beta_2 a$, beyond
627 which it will decay to zero. Therefore, this pulse may be implemented to compensate for the medium's losses
628 when the width of the medium is a given parameter.

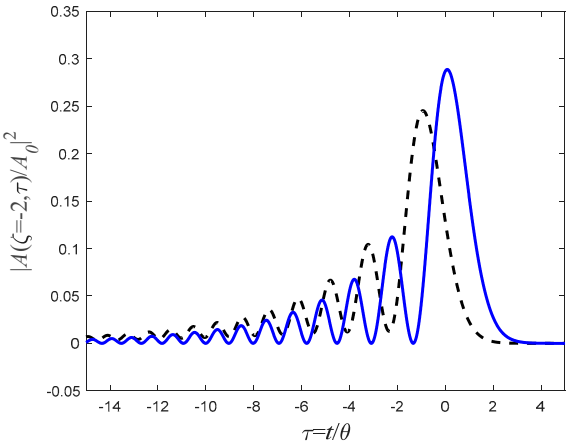

629

630 Fig. 28: Same as Fig.27, but for pulse (97) with $\eta/\theta = 0.2$ and $a = 0.1/\theta$.

631

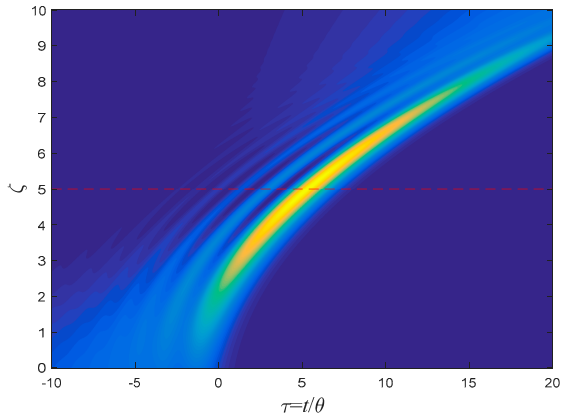

632

633 Fig.29: Same as Fig.2 but for the intensity ($|A(t,z)|^2$) of the pulse presented by Eq.(97) for $a = 0.2/\theta$ and
634 $\eta/\theta = 1$. The horizontal line corresponds for the maximum intensity distance $z = \eta/\beta_2 a$.

635

636

637 **9. Discussions and Conclusions**

638

639 Dispersive media can have destructive effect on ultrashort pulses even at relatively short distances.

640 This chapter shows that almost any pulse shape in most practical scenarios can be formulated in a pulse form,
641 whose propagation in dispersive medium has *an exact analytical expression*.

642 Therefore, there is no need to restrict the analysis of pulse propagation in dispersive medium to Gaussian pulses
643 or to numerical analysis. Thus, almost any shape and form of pulses can be analyzed *analytically*. This is the
644 main result and main conclusion of this chapter.

The experimentalist can choose from the multiple examples presented in this chapter to predict the distortions that the relevant pulse would experience.

In particular, if the pulses were generated by a mode-locked laser then a Gaussian pulses is a good approximation. However, if there is an asymmetry between the pulse's rise and fall times (as in Q-switch lasers), then the experimentalist can use the smooth exponential pulses (section 6.6) to predict the pulse's distortions.

Similarly, in modern optical communications channels, the data signals consist of multiple pulses, which mostly belong to two categories: rectangular and Nyquist pulses. Both types of pulses are presented in this chapter, however, these pulses are both discontinuous: the former is discontinuous in the time domain while the latter is discontinuous in the frequency domain. In practical cases the signals are always continuous (in both time and frequency domains). Therefore, the experimentalist or the engineer can measure the pulse's rise time and apply the smooth rectangular pulses (section 6.2) to the relevant system to predict the pulse's distortion in the fiber. Similarly, Nyquist-sinc pulses with smooth spectrum (section 7.2) can be used to simulate real systems, which are based on Nyquist-since pulses. The exact dispersion's distortion can be evaluated without the need for approximations or for numerical analysis.

Moreover, this chapter demonstrates that any singular pulse can be replaced with a smooth pulse, whose evolution in dispersive medium can be formulated in exact analytical form.

Besides the usage of this chapter as a handbook of analytical expressions for pulses' propagations in dispersive medium, there are several new findings. The main ones are: Exact analytical expression for the evolution (in dispersive medium) of chirped rectangular pulses, which can converge to extremely narrow pulses; analytical approximation for the evolution of Super-Gaussian pulses in dispersive medium; a physical realization of Nyquist Sinc Pulse, i.e., pulses with smooth-rectangular spectrum; and a physical realization of attenuation compensating Airy pulse.

Appendix A: Proof of Eq.(3)

The spectral transfer function of the medium is

$$H(\omega)=\exp\left(i\beta_2 z\omega^2/2\right), \tag{A1}$$

i.e., for the incident signal $A(t,z=0)=A_0\exp(\pm i\omega t)$ the signal after a distance of z is simply $A(t,z>0)=A_0H(\omega)\exp(\pm i\omega t)$. In general, let $A(\omega,z)=F\{A(t,z)\}$ be the Fourier transform of $A(t,z)$ then

$$A(\omega,z>0)=H(\omega)A(\omega,0). \tag{A2}$$

Since the Fourier transform of a product is a convolution of the Fourier transforms, then the application of the Fourier transform on (A2) yields

$$A(t,z)=\int_{-\infty}^{\infty}K(t-t',z)A(t',0)dt' \tag{A3}$$

where

$$K(t,z)=F\{H(\omega)\}=(-2\pi i\beta_2 z)^{-1/2}\exp\left(-i\frac{t^2}{2\beta_2 z}\right) \tag{A4}$$

is the Fourier transform of $H(\omega)$.

Appendix B: Proof of Eq.(6)

Let

$$A'(t,z=0)=\exp(i\omega_0 t)A(t,0) \tag{B1}$$

and let us further assume that

$$A(t,z)=\int_{-\infty}^{\infty}K(t-t',z)A(t',0)dt' \tag{B2}$$

is given. Then

$$A'(t,z)=\int_{-\infty}^{\infty}K(t-t',z)\exp(i\omega_0 t')A(t',0)dt', \tag{B3}$$

which, after some calculatations can be rewritten as

$$A'(t,z)=\exp\left(i\frac{\beta_2 z\omega_0^2}{2}+i\omega_0 t\right)(-2\pi i\beta_2 z)^{-1/2}\int_{-\infty}^{\infty}\exp\left(-i\frac{[t'-(t+\beta_2 z\omega_0)]^2}{2\beta_2 z}\right)A(t',0)dt' \tag{B4}$$

Using (B2) and (A4) then Eq.(B4) is simply

$$A'(t,z>0)=\exp\left(i\frac{\beta_2}{2}\omega_0^2 z+i\omega_0 t\right)A(t+\beta_2\omega_0 z,z) \tag{B5}$$

Appendix C: Proof of Eq.(10)

Let

$$A'(t,0)=\exp(-iqt^2)A(t,0) \tag{C1}$$

and let us further assume that

$$A(t,z)=\int_{-\infty}^{\infty}K(t-t',z)A(t',0)dt' \tag{C2}$$

is given. Then

$$A'(t,z)=\int_{-\infty}^{\infty}(-2\pi i\beta_2 z)^{-1/2}\exp\left(-i\frac{(t-t')^2}{2\beta_2 z}\right)A(t',0)\exp(-iqt'^2)dt' \tag{C3}$$

which after some algebra can be written as

$$A'(t,z)=\left(\frac{1+2\beta_2 zq}{1+2\beta_2 zq}\right)^{1/2}\frac{\exp\left(-i\dfrac{t^2}{2\beta_2 z+1/q}\right)}{(-2\pi i\beta_2 z)^{1/2}}\int_{-\infty}^{\infty}\exp\left(-i\left(\frac{1+2\beta_2 zq}{2\beta_2 z}\right)\left(t'-\frac{t}{1+2\beta_2 zq}\right)^2\right)A(t',0)dt' \qquad \text{(C4)}$$

Using (C2), Eq.(C4) can simply be rewritten as

$$A'(t,z)=(1+2\beta_2 zq)^{-1/2}\exp\left(-i\frac{t^2}{2\beta_2 z+1/q}\right)A\left(\frac{t}{1+2\beta_2 zq},\frac{z}{1+2\beta_2 zq}\right). \qquad \text{(C5)}$$

References

1. Zevallos, M. E.; Gayen, S. K. ; Das, B. B.; Alrubaiee M., and Alfano R. R. "Picosecond Electronic Time-Gated Imaging of Bones in Tissues" IEEE J. of Selected topics in Quantum Electronics, 5, 1999
2. Gayen S. K. and Alfano R. R., "Emerging optical biomedical imaging techniques," Opt. Photon. News, 7, 17–22, 1996
3. Das B. B., Yoo K. M., and Alfano R. R., "Ultrafast time-gated imaging in thick tissues: A step toward optical mammography," Opt. Lett., 18, 1092–1094, 1993.
4. Marom D.M., Sun P.C., Fainman Y., "Communication with ultrashort pulses and parallel-to-serial and serial-to-parallel converters", Conference Proceedings. LEOS '97. 10th Annual Meeting IEEE Lasers and Electro-Optics Society (1997)
5. Amiri I. S., Ahmad H., "Optical Soliton Communication Using Ultra-Short Pulses", Springer (2015)
6. Yamaoka Y., Harada Y., Sakakura M., Minamikawa T., Nishino S., Maehara S., Hamano S., Tanaka H., and Takamatsu T., "Photoacoustic microscopy using ultrashort pulses with two different pulse durations", Optics Express Vol. 22, 17063-17072 (2014)
7. Gibbs H. C., Arne Y. B. , Alvin C. L., and Yeh T., "Imaging embryonic development with ultrashort pulse microscopy", Optical Engineering 53(5), 051506 (May 2014)
8. "Technical Note: The Effect of Dispersion on Ultrashort Pulses", Newport Corporation (2018), available online: https://www.newport.com/n/the-effect-of-dispersion-on-ultrashort-pulses
9. Sindhu T.G., Bisht P.B., Rajesh R.J., Satyanarayana M.V., "Effect of higher order nonlinear dispersion on ultrashort pulse evolution in a fiber laser", Microwave Opt. Technol. Lett. 28: 196–198, 2001
10. Wang W., Liu Y., Xi P., Ren Q., "Origin and effect of high-order dispersion in ultrashort pulse multiphoton microscopy in the 10 fs regime." Appl Opt. 49(35):6703-9. (2010)
11. Granot E., "Fundamental dispersion limit for spectrally bounded On-Off-Keying communication channels and its implications to Quantum Mechanics and the Paraxial Approximation", Europhys. Lett. 100, 44004 (2012);
12. Granot E., "Information Loss in Quantum Dynamics", a chapter in the book *Advanced Technologies of Quantum Key Distribution* (INTECH, Rijeka, 2017).
13. Wollenhaupt M., Assion A., and Baumert T., " Femtosecond Laser Pulses: Linear Properties, Manipulation, Generation and Measurement", Chap. 12 in Hanbookd of Laser and Optics, Ed. F. Träger, Springer, New-York (2007)
14. Agrawal G. P., Fiber-Optic Communications Systems, Third Edition. John Wiley & Sons, Inc. (2002)
15. Crank J., *The Mathematics of Diffusion*, Clarendon Press, Oxford 1975
16. Ali R., Y. Hamza M., " Propagation behavior of super-Gaussian pulse in dispersive and nonlinear regimes of optical communication systems", International Conference on Emerging Technologies (ICET 2016)
17. Anderson D. and Lisak M., "Propagation characteristics of frequency-chirped super-Gaussian optical pulses," Opt. Lett. 11, 569-571 (1986)
18. Zhang L., Li C., Zhong H., Xu C., Lei D., Li Y., and Fan D., "Propagation dynamics of super-Gaussian beams in fractional Schrödinger equation: from linear to nonlinear regimes" Opt. Express 24,14406-14418 (2016)
19. Moshinsky M., "Diffraction in time," Phys. Rev. 88, 625–631 (1952).

20. del Campo A., Garcia-Calderon G., and Muga J. G., "Quantum Transients," Phys. Rep.. 476, 1–50 (2009).
21. Berry M. V., "Quantum fractals in boxes", J. Phys. A: Math. Gen. 29, 6617–6629 (1996)
22. Granot E. and Marchewka A., "Generic Short-Time Propagation of Sharp-Boundaries Wave Packets" Europhysics Letters 72, 341-347 (2005).
23. Granot E., Luz E. and Marchewka A., "Generic pattern formation of sharp-boundaries pulses propagation in dispersive media", Journal of the Optical Society of America B 29, 763-768 (2012);
24. Granot E. and Marchewka A., "Emergence of currents as a transient quantum effect in nonequilibrium systems" Physical Review A 84, 032110-032115 (2011)
25. Marciano S., Ben-Ezra S., and Granot E., "Eavesdropping and Network Analyzing Using Network Dispersion" Appl. Phys. Res., 7, 27 (2015)
26. Soto M.A., Alem M., Shoaie M.A., Vedadi A., Brès C-S, Thévenaz L., and Schneider T., "Optical sinc-shaped Nyquist pulses of exceptional quality " Nature Communications 4, Article number: 2898 (2013)
27. Schmogrow R., Bouziane R., Meyer M., Milder P. A., Schindler P. C., Killey R. I., Bayvel P., Koos C., Freude W., and Leuthold J., " Real-time OFDM or Nyquist pulse generation – which performs better with limited resources? ", Optics Express 20, B543 (2012)
28. Hirooka, T., Ruan, P., Guan, P. & Nakazawa, M. Highly dispersion-tolerant 160 Gbaud optical Nyquist pulse TDM transmission over 525 km. Opt. Express 20, 15001–15007(2012).
29. Hirooka, T. & Nakazawa, M. Linear and nonlinear propagation of optical Nyquist pulses in fibers. Opt. Express 20, 19836–19849 (2012).
30. Schmogrow, R. et al. 512QAM Nyquist sinc-pulse transmission at 54 Gbit/s in an optical bandwidth of 3 GHz. Opt. Express 20, 6439–6447 (2012).
31. Bosco, G., Carena, A., Curri, V., Poggiolini, P. & Forghieri, F. Performance limits of Nyquist-WDM and CO-OFDM in high-speed PM-QPSK systems. IEEE Phot. Technol. Lett. 22, 1129–1131 (2010).
32. Berry M. V., Balázs, N. L. "Nonspreading wave packets". American Journal of Physics. 47, 264–267 (1979).
33. Siviloglou G. A., Broky J., Dogariu A., Christodoulides D.N., "Observation of Accelerating Airy Beams". Phys. Rev. Lett. 99, 213901. (2007).
34. Bandres, M. A. "Accelerating beams". Opt. Lett. 34 (24): 3791–3793 (2009).
35. Abramowitz M. and Stegun A., Handbook of Mathematical Functions (Dover, 1965).
36. Siviloglou G. A. and Christodoulides D. N., "Accelerating finite energy Airy beams", Opt. Lett. 32, 979 (2007)
37. Preciado, M. A.; Dholakia, K.; Mazilu, M. (2014-08-15). "Generation of attenuation-compensating Airy beams". Optics Letters. 39 (16): 4950–4953.
38. Preciado M. A. and Sugden K., "Proposal and design of airy-based rocket pulses for invariant propagation in lossy dispersive media" Opt. Lett. 37, 4970– 4972 (2012).